Article

Molecular Cell

CLOCK Acetylates ASS1 to Drive Circadian Rhythm of Ureagenesis

Graphical Abstract

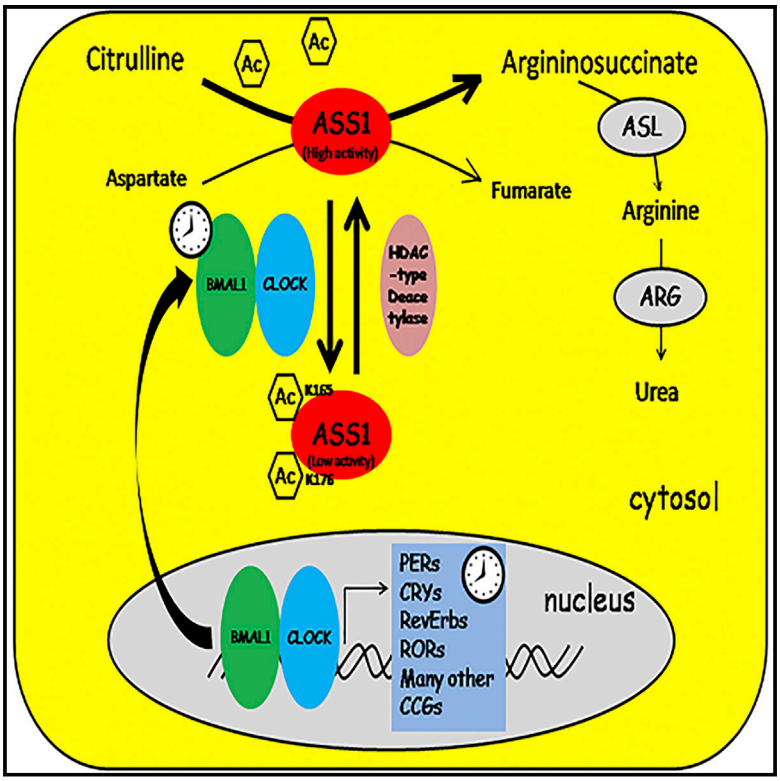

Highlights

- CLOCK acetylates metabolic enzymes to modulate their activity
- CLOCK drives the cycle of acetylation and activation of metabolic enzymes
- Interaction between CLOCK and metabolic enzymes is rhythmic
- Arginine biogenesis and ureagenesis are rhythmically controlled by ASS1 acetylation

Authors

Ran Lin, Yan Mo, Haihong Zha, ..., Ying Xu, Yue Xiong, Kun-Liang Guan

Correspondence

rlin@fudan.edu.cn (R.L.), yxiong@email.unc.edu (Y.X.), kuguan@ucsd.edu (K.-L.G.)

In Brief

Lin et al. reported that CLOCK acetylates ASS1 to inactivate its function in arginine biosynthesis. ASS1 acetylation by CLOCK exhibits rhythmicity, possibly caused by rhythmic interaction between CLOCK and ASS1, leading to the cycle of ASS1 activation. Two more enzymes, NDUFA9 and IMPDH2, were recognized as acetylation substrates of CLOCK.

Lin et al., 2017, Molecular Cell 68, 198–209
October 5, 2017
https://doi.org/10.1016/j.molcel.2017.09.008

CellPress

CellPress

Molecular Cell
Article

CLOCK Acetylates ASS1 to Drive Circadian Rhythm of Ureagenesis

Ran Lin,[1,6,*] Yan Mo,[1] Haihong Zha,[2] Zhipeng Qu,[3] Pancheng Xie,[3] Zheng-Jiang Zhu,[2] Ying Xu,[3] Yue Xiong,[1,4,*] and Kun-Liang Guan[1,5,*]

[1]State Key Laboratory of Genetic Engineering, Collaborative Innovation Center for Genetics and Development, School of Life Sciences, Molecular and Cell Biology Laboratory, Institute of Biomedical Sciences, Shanghai Medical College of Fudan University, Shanghai 200032, China

[2]Interdisciplinary Research Center on Biology and Chemistry and Shanghai Institute of Organic Chemistry, Chinese Academy of Sciences, Shanghai 200032, China

[3]Cam-Su Genomic Resource Center, Soochow University, Suzhou 215123, China

[4]Department of Biochemistry and Biophysics, Lineberger Comprehensive Cancer Center, University of North Carolina at Chapel Hill, Chapel Hill, NC 27599, USA

[5]Department of Pharmacology and Moores Cancer Center, University of California, San Diego, La Jolla, CA 92093, USA

[6]Lead Contact

*Correspondence: rlin@fudan.edu.cn (R.L.), yxiong@email.unc.edu (Y.X.), kuguan@ucsd.edu (K.-L.G.)

https://doi.org/10.1016/j.molcel.2017.09.008

SUMMARY

In addition to responding to environmental entrainment with diurnal variation, metabolism is also tightly controlled by cell-autonomous circadian clock. Extensive studies have revealed key roles of transcription in circadian control. Post-transcriptional regulation for the rhythmic gating of metabolic enzymes remains elusive. Here, we show that arginine biosynthesis and subsequent ureagenesis are collectively regulated by CLOCK (circadian locomotor output cycles kaput) in circadian rhythms. Facilitated by BMAL1 (brain and muscle Arnt-like protein), CLOCK directly acetylates K165 and K176 of argininosuccinate synthase (ASS1) to inactivate ASS1, which catalyzes the rate-limiting step of arginine biosynthesis. ASS1 acetylation by CLOCK exhibits circadian oscillation in human cells and mouse liver, possibly caused by rhythmic interaction between CLOCK and ASS1, leading to the circadian regulation of ASS1 and ureagenesis. Furthermore, we also identified NADH dehydrogenase [ubiquinone] 1 alpha subcomplex subunit 9 (NDUFA9) and inosine-5′-monophosphate dehydrogenase 2 (IMPDH2) as acetylation substrates of CLOCK. Taken together, CLOCK modulates metabolic rhythmicity by acting as a rhythmic acetyl-transferase for metabolic enzymes.

INTRODUCTION

Like many other aspects of human physiology, metabolism exhibits circadian rhythm. Such rhythm is tightly controlled by the internal circadian clock, which coordinates metabolic events to particular phases within a 24 hr light/dark cycle associated with diurnal environmental changes (e.g., food intake and physical activity). Therefore, metabolic disorders (e.g., obesity, diabetes, and cardiovascular diseases) frequently occur when the internal circadian clock is misaligned with external environment, as seen in jet-lag travelers and rotational shift workers (Reddy and O'Neill, 2010). Severe impairments of glucose homeostasis and lipid metabolism are also observed in clock-defected mice (Lamia et al., 2008; Rudic et al., 2004; Shimba et al., 2011; Turek et al., 2005) or fruit flies (Xu et al., 2008). Oncogenic lesions like neuroblastoma and hepatocellular carcinoma can develop from metabolic abnormality in clock-perturbed mice (Altman et al., 2015; Kettner et al., 2016).

The internal self-sustained circadian clock is hardwired in every peripheral tissue, consisting of interconnected negative feedback loops (Chong et al., 2012; Partch et al., 2014). In principle, two transcription factors, CLOCK (circadian locomotor output cycles kaput) and BMAL1 (brain and muscle Arnt-like protein 1, also known as aryl hydrocarbon receptor nuclear translocator-like protein 1 [ARNTL]), assemble into a tightly intertwined heterodimer (Huang et al., 2012) to initiate the transcription of a large set of target genes (called clock-controlled genes [CCGs]), including period (encoding PER1/2/3) and cryptochrome (encoding CRY1/2). Later, PER and CRY also assemble into a heterodimer and enter the nucleus, where they suppress the activity of CLOCK/BMAL1 and therefore attenuate their own transcription. Because the turnover of PER and CRY is also rhythmic, CLOCK/BMAL1 is then re-activated to start a new cycle of transcription. One such cycle spans ~24 hr to constitute the circadian cycle.

Rhythmic CCG expression supports the temporal governing of physiology in peripheral tissues. Indeed, cycling of mRNA is detected in ~10%–20% of the genes by which numerous metabolic enzymes are encoded. In addition, mRNA translation and protein turnover might also be under clock control (Feng and Lazar, 2012). Moreover, the rhythmicity of metabolism is also shaped by post-translational modification of metabolic enzymes. Accumulating evidence indicates that acetylation is an

essential mechanism to regulate metabolic enzymatic activity (Guan and Xiong, 2011; Zhao et al., 2010). Proteomic studies have identified a broad range of enzymes involved in glucose, amino acids, and fatty acid metabolism showing clock-dependent oscillation of acetylation (Masri et al., 2013). This is exemplified by fatty acid elongation factor acetyl-CoA synthase (AceCS1), whose acetylation cycle is driven by SIRT1 (Sahar et al., 2014), while the acetylation of certain other mitochondrial metabolic enzymes, ornithine transcarbamylase (OTC), manganese-dependent superoxide dismutase (MnSOD), and isocitrate dehydrogenase 2 (IDH2), is rhythmically targeted by SIRT3 (Peek et al., 2013). In contrast to deacetylases, the knowledge on rhythmic acetyl-transferase is relatively limited.

As an essential transcription factor in circadian feedback loop, CLOCK was also identified as a histone acetyl-transferase (HAT) and its HAT activity on H3/H4 is indispensable for rhythmic expression of CCGs, possibly through epigenetic regulation (Doi et al., 2006). It remains an open question whether CLOCK has non-histone substrates.

In the present study, we discovered arginine biosynthesis pathway metabolites (arginine, argininosuccinate, and citrulline) to be collectively altered by CLOCK depletion in human cells. Facilitated by BMAL1, CLOCK directly acetylates K165 and K176 of argininosuccinate synthase 1 (ASS1) in vitro and in vivo and inhibits this rate-limiting enzyme in arginine biosynthesis and the subsequent ureagenesis. ASS1 acetylation by CLOCK exhibits circadian oscillation in human cells and mouse liver, possibly caused by rhythmic interaction between CLOCK and ASS1, leading to the rhythmic inactivation of ASS1 and oscillation of ureagenesis. Furthermore, we identified two more metabolic enzymes, NDUFA9 (NADH dehydrogenase [ubiquinone] 1 alpha subcomplex subunit 9) and IMPDH2 (inosine-5′-monophosphate dehydrogenase 2), as circadian acetylation substrates of CLOCK. IMPDH2 also shows rhythmic interaction with CLOCK. Our findings support a model that CLOCK is a rhythmic and functional acetyl-transferase for metabolic enzymes and contributes to the cell-autonomous circadian regulation of metabolism.

RESULTS

Hyperactivation of Arginine Biosynthesis Pathway and Ureagenesis in CLOCK-Depleted Cells

U2OS osteosarcoma cells, a model commonly used in study of the cell-autonomous circadian clock, were used to explore possible roles of CLOCK in the circadian regulation of metabolic pathways. Two independent clones of U2OS cell lines with CLOCK knockout were generated by the CRISPR/Cas9 genomic editing system, each harboring a homozygous deletion in the third exon within the coding sequence of *clock* gene (Figure S1A). Consistent with the known function of CLOCK in circadian rhythms, deletion of CLOCK in U2OS cells disrupted the normal circadian rhythms reflected by the lack of rhythmic expression of period 2 mRNA (Figure S1B) and period 2 and RevErb-α protein (Figure S1C).

Targeted high-throughput metabolomic profiling was conducted in one of the clones (KO#1) by liquid chromatography-mass spectrometry (LC-MS) with multiple reaction monitoring (MRM) analysis (Figure S1D). A large number of metabolites were identified to be altered by CLOCK deletion (Figure 1A; Table S1). Within this range, metabolites of arginine biosynthesis pathway (citrulline, argininosuccinate, and arginine) (Figure 1A) were enriched. The abundance of arginine and its precursor, argininosuccinate, were both elevated, while citrulline level was reduced in CLOCK KO#1 U2OS cells (Figure 1B, left), indicating the upregulation of arginine biosynthesis in CLOCK KO cells. A similar change of arginine and argininosuccinate was detected in CLOCK KO#2 U2OS cells by targeted LC-MS analyses (Figure 1B, right).

Arginine could be converted by Arginase 1/2 to produce urea, the last step of ureagenesis that the human body employs for ammonia detoxification. Despite the lack of OTC, the last enzyme to complete the urea cycle (data not shown), a significant amount of urea was still detected in U2OS cells by gas chromatography-mass spectrometry (GC-MS), and the intracellular urea content was elevated in both CLOCK KO#1 and #2 U2OS cells (Figure 1C). Ureagenesis is largely restrained in liver where an intact urea cycle exists. We examined the HL-7702 (also named L-02) cells, which are immortalized human hepatocytes, and observed the rhythmic cycle of period 2 and RevErb-α expression at protein levels, similar to those in U2OS cells (Figure S1E). Like the CLOCK KO U2OS cells, HL-7702 cells with efficient CLOCK knockdown by two independent small interfering RNAs (siRNAs) (Figure S1F) displayed elevation of urea content (Figure 1D).

Binding with BMAL1 is required for the functions of CLOCK as either transcription factor or acetyl-transferase (Doi et al., 2006). Consistently, knockdown of BMAL1 by two independent siRNAs (Figure S1F) also resulted in hyper-activation of ureagenesis in HL-7702 cells (Figure 1D). Together, the above data show that ablation of the CLOCK/BMAL1 central clock increases arginine biosynthesis and ureagenesis, supporting the circadian regulation of these metabolic processes.

CLOCK and BMAL1 Promote ASS1 Acetylation

The arginine biosynthesis pathway consists of two steps: ligation of citrulline and aspartate to argininosuccinate catalyzed by ASS1, and breakdown of argininosuccinate to produce arginine and fumarate catalyzed by argininosuccinate lyase (ASL). As the pathway was enhanced by CLOCK depletion, we examined the expression of both ASS1 and ASL. At either mRNA (Figure S2A) or protein level (Figure S2B), similar amounts of ASS1 and ASL were detected in CLOCK KO#1 and KO#2 cells, compared with wild-type (WT) control cells. Therefore, CLOCK may regulate these enzymes at post-translational levels.

Ectopic co-expression of Flag-tagged ASL and CLOCK in HEK293T cells did not result in altered acetylation in immunoprecipitated ASL-Flag (Figure S2C). In contrast, co-expression of Flag-tagged ASS1 and CLOCK caused an obvious increase of acetylation in immunoprecipitated ASS1-Flag (Figure 2A). This induction of acetylation was also detected when ASS1-Flag was co-expressed together with BMAL1 in HEK293T cells (Figure 2A). Expression of Flag-tagged ASS1 in CLOCK KO#1 and KO#2 U2OS cells resulted in dramatically reduced acetylation, compared with WT U2OS cells (Figure 2B). In addition,

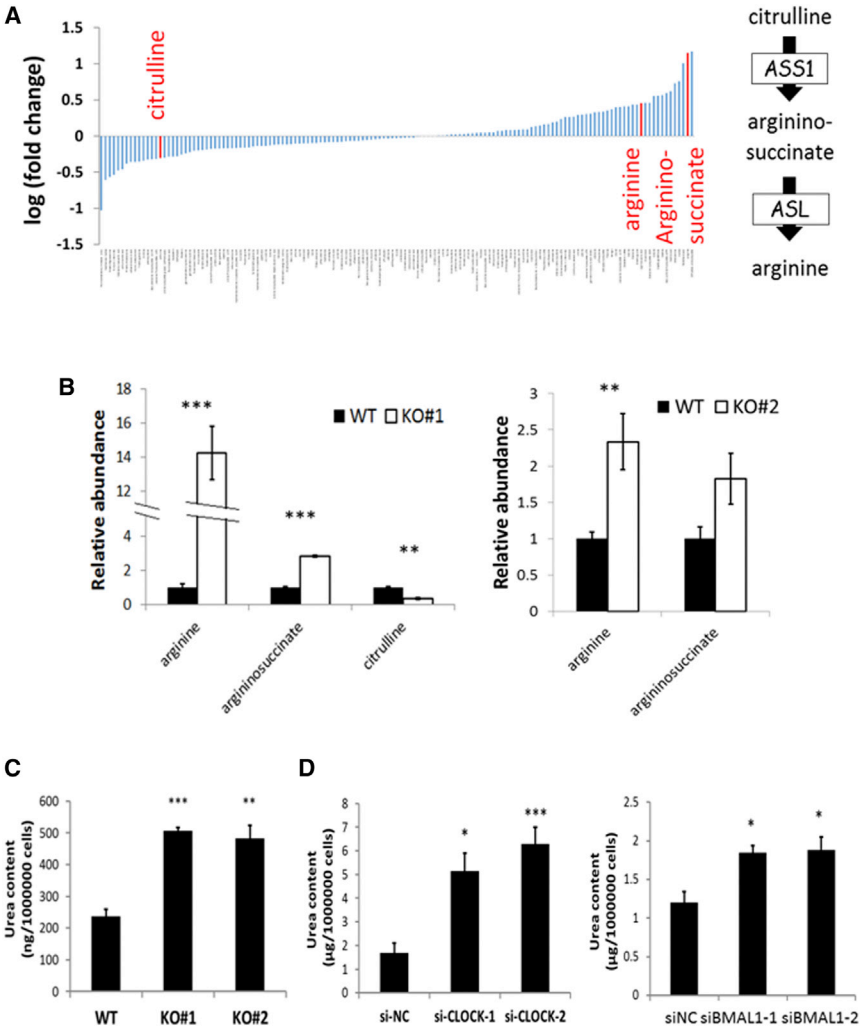

Figure 1. Metabolic Profiling Identifies Alteration of Arginine Biosynthesis Pathway in CLOCK Knockout U2OS Cells

(A) Alteration in metabolites in CLOCK KO U2OS cells. Left: mean fold change of metabolites analyzed in WT versus CLOCK KO#1 U2OS cells, with arginine biosynthesis pathway components highlighted. Right: depiction of metabolites and enzymes in arginine biosynthesis pathway.

(B) Relative abundance of arginine biosynthesis pathway metabolites is elevated in CLOCK KO U2OS cells compared with WT cells. The relative abundance of citrulline, argininosuccinate, and arginine was determined by the metabolic profiling (left, n = 3 for each bar) in WT and CLOCK KO#1 U2OS cells, or by an independent LC-MS test in WT and CLOCK KO#2 U2OS cells (right, n = 6 for each bar).

(C) Urea content is elevated in U2OS KO U2OS cells. Urea content in whole cell metabolite extract from WT and CLOCK KO#1 and KO#2 U2OS cells was determined by GC-MS. Urea chemical was used as a standard in the GC-MS analysis, n = 3 for each bar.

(D) Knockdown of CLOCK or BMAL1 increases urea content in HL-7702 hepatocytes. The immortalized HL-7702 hepatocytes were transfected with siRNA negative control (NC) or two independent siRNAs targeting CLOCK (left) or BMAL1 (right). Urea content in whole cell metabolite extract was determined by GC-MS. n = 3 for each bar.

Data are graphed as the mean ± SEM, *p < 0.05, **p < 0.01, ***p < 0.001.

See also Figure S1 and Table S1.

endogenous ASS1 showed a reduced acetylation in CLOCK KO#1 U2OS cells, compared with ASS1 in WT cells (Figure 2C). In CLOCK KO#1 U2OS cells, stable ectopic expression of WT CLOCK, but not the mutant CLOCK without acetyl-transferase activity (Doi et al., 2006), restored acetylation of the co-expressed ASS1-Flag (Figure 2D). These data suggest that CLOCK promotes ASS1 acetylation.

The effect of CLOCK on ASS1 acetylation was further examined in HL-7702 hepatocytes. Knockdown of CLOCK by two independent siRNAs in HL-7702 cells largely suppressed acetylation of endogenous ASS1 detected in immunoprecipitation (Figure 2E). The effect of BMAL1 was also tested in U2OS cells. BMAL1 knockdown significantly reduced acetylation of the immunoprecipitated ASS1-Flag (Figure 2F). The regulation of ASS1 acetylation by CLOCK implies a direct association of CLOCK with ASS1, which was supported by the detection of endogenous CLOCK in immunoprecipitates of endogenous ASS1 in U2OS cells (Figure 2G). ASS1 protein was exclusively detected in cytosol of U2OS cells, while CLOCK distributed in both cytosol and nuclear compartments (Figure S6E); hence, CLOCK likely promotes ASS1 acetylation in cytosol.

To further understand the regulation of ASS1 acetylation, we explored deacetylases that may regulate ASS1. Trichostatin A (TSA) is a potent inhibitor toward both class I and II deacetylase (HDACs) (Yoshida et al., 1990). The acetylation of ASS1-Flag was enhanced in WT U2OS cells treated with TSA (Figure S2D). Sirtinol specifically inhibits the two major cytosolic Sirtuins (class III deacetylase), SIRT1 and SIRT2 (Grozinger et al., 2001). Treatment with Sirtinol at various doses and durations did not change the acetylation of ASS1-Flag in WT U2OS cells (Figure S2E). The above observations suggest that HDAC, but not Sirtuin, is responsible for ASS1 deacetylation in cytosol.

CLOCK Directly Acetylates ASS1 at K165 and K176 Residues

The findings described above suggest that ASS1 might be a substrate of the CLOCK acetyl-transferase. This possibility was explored by in vitro acetylation assay with recombinant ASS1 and truncated CLOCK containing the C-terminal acetyl-transferase domain (CLOCKΔN) (Doi et al., 2006), which was expressed and purified from *E. coli* (Figure S3A). In the acetylation reaction system containing acetyl-CoA, CLOCKΔN acetylated H3 in a dose-dependent manner, confirming the previous report that CLOCK has histone acetyl-transferase activity (Doi

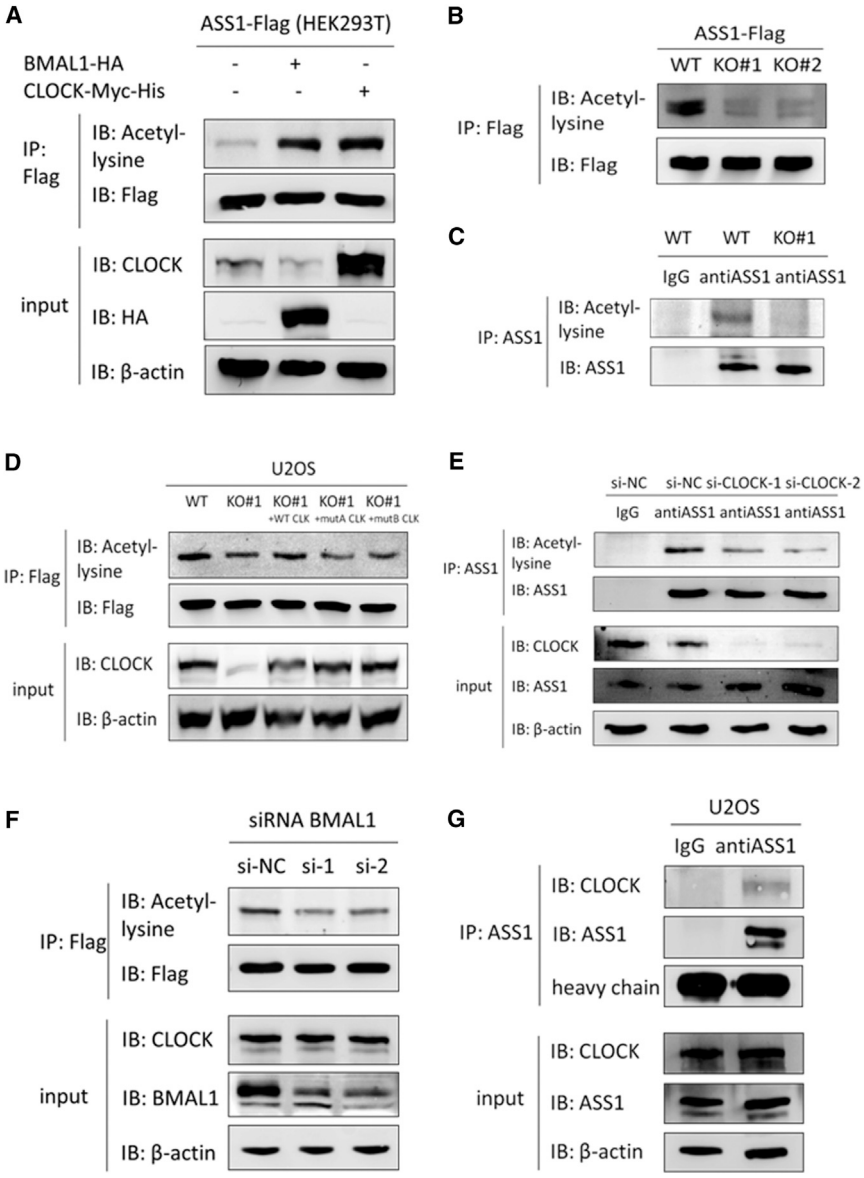

Figure 2. CLOCK Regulates ASS1 Acetylation

(A) Acetylation of ectopically expressed ASS1 is elevated by co-expression of CLOCK or BMAL1. Flag-tagged ASS1 was transfected into HEK293T cells together with Myc-tagged CLOCK or HA-tagged BMAL1. Acetylation was determined by western blotting with anti-acetyl-lysine antibody in immunoprecipitate of Flag.

(B) Acetylation of ectopically expressed ASS1 is declined in CLOCK KO U2OS cells. Flag-tagged ASS1 was transfected into WT, CLOCK KO #1, and #2 U2OS cells. Acetylation was determined by western blotting with anti-acetyl-lysine antibody in immunoprecipitate of Flag.

(C) Acetylation of endogenous ASS1 is reduced in CLOCK KO U2OS cells. Endogenous ASS1 was immunoprecipitated from WT or CLOCK KO#1 U2OS cells and its acetylation was determined by western blotting with anti-acetyl-lysine antibody.

(D) The acetyl-transferase activity of CLOCK is required to restore ASS1 acetylation in CLOCK KO U2OS cells. Flag-tagged ASS1 was transfected into U2OS WT cells, CLOCK KO#1 cells, and the KO#1 cells with ectopic expression of CLOCK WT, mutant A, or mutant B. Acetylation was determined by western blotting with anti-acetyl-lysine antibody in immunoprecipitate of Flag.

(E) CLOCK knockdown reduces acetylation of endogenous ASS1 in HL-7702 cells. The immortalized HL-7702 hepatocytes were transfected with siRNA negative control (NC) or two independent siRNAs targeting CLOCK. Endogenous ASS1 was immunoprecipitated and its acetylation was determined by western blotting with anti-acetyl-lysine antibody.

(F) BMAL1 knockdown reduces acetylation of ectopically expressed ASS1. U2OS cells were transfected with Flag-tagged ASS1 together with siRNA negative control (NC) or two independent siRNAs targeting BMAL1. Acetylation was determined by western blotting with anti-acetyl-lysine antibody in immunoprecipitate of Flag.

(G) CLOCK binds to ASS1 in U2OS cells. CLOCK protein was detected by western blotting in immunoprecipitate of endogenous ASS1 in WT U2OS cells.

See also Figure S2.

et al., 2006) (Figure S3B). In the same reaction system, ASS1 was also acetylated by CLOCKΔN in dose-dependent (Figure 3A) and time-dependent (Figure 3B) manners. To exclude the possibility that ASS1 was acetylated by a non-specific factor co-purified from *E. coli*, ASS1 was incubated without CLOCKΔN and no increase of acetylation was observed, demonstrating the in vitro acetylation was caused by CLOCKΔN (Figure S3C).

To identify residues in ASS1 acetylated by CLOCK, recombinant ASS1 after in vitro CLOCK acetylation or control condition was analyzed by LC-tandem MS (LC-MS/MS). Several lysine residues were identified to be acetylated with different intensity. The top rank residues included K165 and K176 (Figures 3C and S3D), which were located in close proximity with substrates (citrulline and aspartate) handling the catalytic center of ASS1 (PDB: 2nz2) (Karlberg et al., 2008) (Figure S3E). These two lysine residues are highly conserved among kingdoms of fungus, plants, insects, and mammals (Figure S3F). The majority of ASS1 acetylation by CLOCK was contributed by K165 and K176, as the mutation of these two lysines to arginine or glutamine almost completely prevented the in vitro acetylation of ASS1 by CLOCKΔN (Figure 3D). In U2OS cells, immunoprecipitated WT ASS1-Flag was detected to be acetylated in WT cells and the ASS1 acetylation was dramatically reduced in CLOCK KO#1/KO#2 cells. Consistent with the in vitro acetylation data, the mutant K165R/K176R ASS1-Flag showed similarly low acetylation in both WT and KO#1/KO#2 cells, supporting ASS1 K165/K176 as the major CLOCK-dependent acetylation sites (Figure 3E).

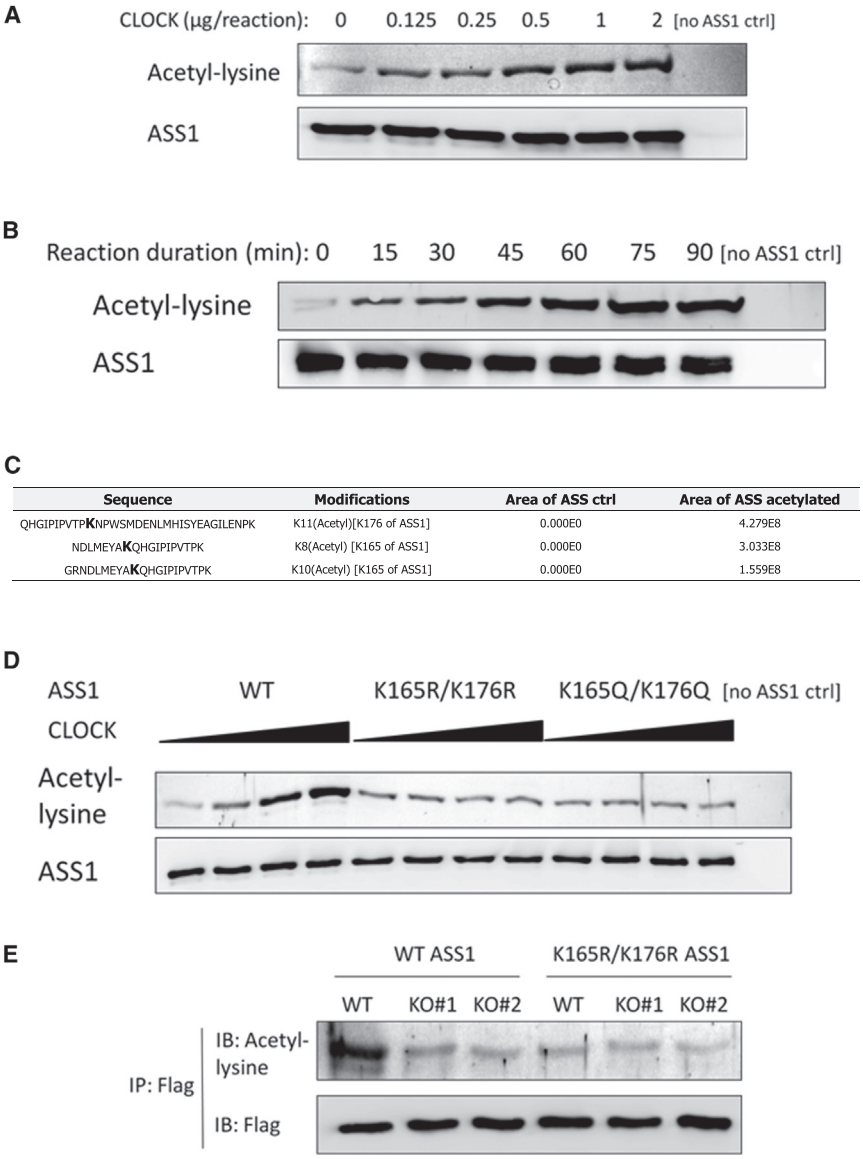

Figure 3. CLOCK Directly Acetylates ASS1 at K165 and K176

(A) CLOCKΔN acetylates ASS1 in a dose-dependent manner in vitro. The *E. coli*-expressed and purified recombinant ASS1 was incubated in vitro with Acetyl-CoA and increasing doses of purified recombinant CLOCKΔN. Acetylation of ASS1 was determined by western blotting with anti-acetyl-lysine antibody.

(B) CLOCKΔN acetylates ASS1 in a time-dependent manner in vitro. The *E. coli*-expressed and purified recombinant ASS1 was incubated in vitro with Acetyl-CoA and purified recombinant CLOCKΔN with varied durations. Acetylation of ASS1 was determined by western blotting with anti-acetyl-lysine antibody.

(C) K165 and K176 in ASS1 are the major acetylation residues by CLOCKΔN. Purified recombinant ASS1 was acetylated in vitro by incubation with Acetyl-CoA and recombinant CLOCKΔN. The acetylated residues in ASS1 were detected by mass spectrometry.

(D) Mutations of K165 and K176 prevent ASS1 acetylation by CLOCKΔN in vitro. Purified recombinant WT, K165R/K176R, or K165Q/K176Q ASS1 was incubated in vitro with acetyl-CoA and increasing doses of purified recombinant CLOCKΔN. Acetylation of WT or mutant ASS1 was determined by western blotting with anti-acetyl-lysine antibody.

(E) CLOCK knockout decreases acetylation of ectopically expressed WT, but not the ASS1 K165R/K176R mutant. Flag-tagged WT or K165R/K176R mutant ASS1 was transfected in WT, CLOCK KO#1, and KO#2 U2OS cells. Acetylation was determined by western blotting with anti-acetyl-lysine antibody in immunoprecipitate of Flag.

See also Figure S3.

Acetylation Inhibits ASS1 Enzymatic Activity

Given that acetylation alters activity of many metabolic enzymes, we assessed the functional consequence of ASS1 acetylation by CLOCK. In vitro acetylation by increasing doses of CLOCKΔN caused reduction of ASS1 activity up to 50%. ASS1 activity was measured by di-phosphate release from the argininosuccinate synthesis reaction (Figure 4A). This ASS1 activity reduction was only detected in WT, but not the K165R/K176R (2KR) or K165Q/K176Q (2KQ) ASS1 mutant, which could not be acetylated by CLOCKΔN (Figure 4B). Notably, glutamine substitution in 2KQ ASS1 reduced enzymatic activity, indicating glutamine substitution may mimic the effect of acetylation to reduce enzyme activity (Figure 4B).

The effect of ASS1 acetylation by CLOCK was also examined in cells. Immunoprecipitated Flag-tagged ASS1 exhibited elevated acetylation when CLOCK was co-expressed in HEK293T cells, and concomitantly, the enzyme activity of ASS1-Flag was reduced under this condition (Figure S4A). In CLOCK KO#1/KO#2 U2OS cells, ectopically expressed and immunoprecipitated ASS1-Flag showed 30% higher activity, compared with the ASS1-Flag expressed in WT U2OS cells (Figure 4C). Compared with WT ASS1, the mutant 2KR ASS1 ectopically expressed in WT U2OS cells had reduced acetylation and elevated enzymatic activity, which was similar to WT ASS1 ectopically expressed in CLOCK KO U2OS (Figure 4D). In addition, ASS1 2KR showed similarly high enzymatic activity whether it was expressed in WT or CLOCK KO cells (Figure 4D). These observations indicate that CLOCK-dependent acetylation inhibits ASS1 enzymatic activity.

To assess the effect of ASS1 acetylation in arginine biosynthesis and ureagenesis, the abundance of arginine and urea was monitored. U2OS cells with *ass1* gene deletion (5 nt and 8 nt deletion in each allele) were generated by CRISPR/Cas9 (Figure S4B, left). Arginine was depleted in these ASS1 KO cells, while ureagenesis was also slightly inhibited. Ectopic expression

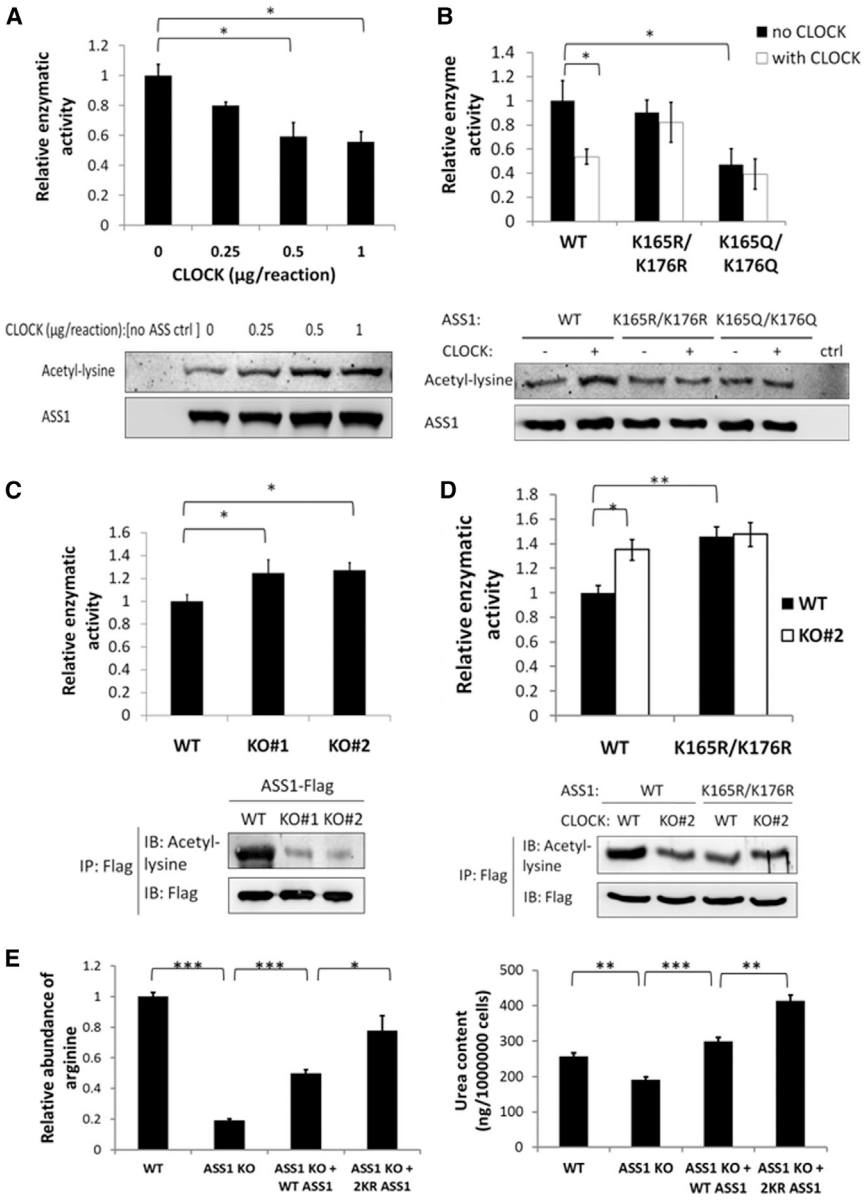

Figure 4. CLOCK Inhibits ASS1 Activity by Acetylation

(A) ASS1 activity is inhibited by CLOCKΔN in a dose-dependent manner in vitro. Purified recombinant ASS1 was incubated with acetyl-CoA and increasing doses of purified recombinant CLOCKΔN. Enzymatic activity of ASS1 was monitored by di-phosphate release from the argininosuccinate synthesis reaction. Top: relative enzymatic activity, n = 3 for each bar. Bottom: western blot detecting ASS1 protein and acetylation of a set of representative samples used in the enzymatic activity assays.

(B) Activity of WT, but not mutant ASS1, is suppressed by CLOCKΔN in vitro. Purified recombinant WT, K165R/K176R, or K165Q/K176Q mutant ASS1 was incubated with acetyl-CoA and purified recombinant CLOCKΔN. Enzymatic activity of WT or mutant ASS1 was monitored by di-phosphate release from the argininosuccinate synthesis reaction. Top: relative enzymatic activity, n = 5 for each bar. Bottom: western blot of a set of representative samples used in enzymatic activity assays.

(C) Activity of ectopically expressed ASS1 is enhanced in CLOCK KO U2OS cells. ASS1-Flag was transfected in WT, CLOCK KO#1, and KO#2 U2OS cells. Enzymatic activity of ASS1 was monitored in immunoprecipitate of Flag by di-phosphate release from the argininosuccinate synthesis reaction. Top: relative enzymatic activity, n = 4 for each bar. Bottom: western blotting detection of ASS1-Flag acetylation and protein levels.

(D) Activity of ectopically expressed WT, but not the acetylation defective mutant ASS1, is enhanced by CLOCK knockout in U2OS cells. Flag-tagged WT or K165R/K176R ASS1 was transfected in WT or CLOCK KO#2 U2OS cells. Enzymatic activity of ASS1 was monitored in immunoprecipitate of Flag by di-phosphate release from the argininosuccinate synthesis reaction. Top: relative enzymatic activity, n = 4 for each bar. Bottom: western blotting detection of acetylation of ASS1-Flag acetylation and protein levels.

(E) Arginine and urea are declined by ASS1 knockout and restored by ectopic expression of ASS1 in U2OS cells. Relative arginine abundance was determined by LC-MS (left, n = 4 for each bar) and urea content was determined by GC-MS (right, n = 3 for each bar) in WT, ASS KO, ASS KO with ectopic expression of WT, or K165R/K176R (2KR) ASS1-Flag U2OS cells as indicated.

Data are graphed as the mean ± SEM, *p < 0.05, **p < 0.01, ***p < 0.001.

See also Figures S4 and S5.

of WT ASS1 in ASS1 KO cells attenuated the reduction of arginine and urea, and ectopic expression of 2KR ASS1 further recovered the decline of arginine and urea (Figures 4E and S4B, right). The above results further support a model that CLOCK-mediated acetylation decreases ASS1 activity.

To explore the functional consequence of CLOCK-dependent ASS1 acetylation at the cellular level, we monitored the cell proliferation. We observed enhanced proliferation of U2OS cells with ectopic overexpression of WT ASS1, but the effect of 2KR ASS1 expression on cell growth was negligible (Figure S5).

Rhythmic Acetylation of ASS1 by CLOCK Governs Circadian Oscillation of Ureagenesis

In the nucleus, CLOCK/BMAL1 controls rhythmic transcription of target genes. We examined whether CLOCK acetylates the cytosolic ASS1 in a rhythmic manner as well. U2OS cells with stable expression of ASS1-Flag were synchronized by dexamethasone (DXM) and then sampled every 4 hr after DXM treatment. Interestingly, we noticed a prominent rhythmic effect of acetylation in immunoprecipitated ASS1-Flag, with peak levels at 24, 48, and 72 hr and trough levels at 36 and 60 hr (Figure 5A). Three more independent repeats were performed and data

quantification confirmed the rhythmic acetylation of ASS1 (Figure S6A). This acetylation cycle was only detected in WT U2OS cells, whereas acetylation of ASS1-Flag expressed in CLOCK KO U2OS cells did not display rhythmicity. Indeed, acetylation of ASS1-Flag at all time points in CLOCK KO cells was as low as the trough acetylation level of ASS1-Flag in WT cells (Figure S6B). K165 and K176 in ASS1 are largely responsible for this rhythmicity because the acetylation of Flag-tagged K165R/K176R ASS1 did not show rhythmicity and was as low as the trough level of WT ASS1 (Figure 5B).

Rhythmic ASS1 acetylation was also detected in HL-7702 hepatocytes. Immunoprecipitated ASS1-Flag from transfected HL-7702 cells exhibited much lower acetylation at 36 hr than 24 hr after DXM synchronization, while ASS1-Flag acetylation was comparably low in CLOCK knockdown HL-7702 cells at both 24 and 36 hr after DXM (Figure 5C). In mouse liver, endogenous ASS1 was immunoprecipitated to detect acetylation at different Zeitgeber times (ZT, an external cue that synchronizes an organism's biological rhythms) within one light/dark cycle with a 4-hr interval. ASS1 acetylation exhibited obvious rhythmicity with peak at ZT12 and troughs at ZT0 and ZT24 (Figure 5D). The ASS1 acetylation was also determined in Bmal1 knockout mouse, in which ZT4 and ZT16 liver ASS1 exhibited comparably low acetylation. In contrast, differential acetylation of liver ASS1 at ZT4 and ZT16 was observed in WT mouse (Figure S6C). These data show that BMAL1, as a key binding partner of CLOCK, also plays a critical role in regulating ASS1 acetylation in mice.

We observed that CLOCK was co-immunoprecipitated with ASS1 in U2OS cells without synchronization (Figure 2G). Next, we tested whether the interaction between ASS1 and CLOCK is regulated. U2OS cells were synchronized with DXM, and ectopically expressed Flag-tagged ASS1 was immunoprecipitated and its acetylation, as well as its interaction with CLOCK, was examined. High levels of CLOCK were detected in the ASS1 immunoprecipitation at 24 and 48 hr after DXM, correlating with the peak time points of ASS1 acetylation. CLOCK was weakly associated with Flag-tagged ASS1 at 36 hr after DXM when ASS1 exhibited lowest acetylation (Figure 5E). The differential binding of CLOCK to ASS1 was also observed in mouse liver. More CLOCK was co-immunoprecipitated with endogenous ASS1 in mouse liver at ZT12, when ASS1 acetylation peaked, whereas less CLOCK-ASS1 interaction was detected at ZT0, when ASS1 acetylation was low (Figure S6D). As CLOCK shuttled between nucleus and cytosol, its sub-cellular distribution was determined at different time points in DXM-synchronized U2OS cells. Although the cytosolic localization of CLOCK was confirmed, the abundance of CLOCK in cytosol and nucleus was similar at different time points. This observation argues against a model that a differential CLOCK subcellular localization contributes to the rhythmic interaction with ASS1 (Figure S6E).

Based on the rhythmicity of ASS1 acetylation, enzymatic activity of ASS1 should also oscillate as acetylation inhibits ASS1 activity. In U2OS cells, ectopically expressed ASS1-Flag had ~20% higher activity at 36 hr after synchronization, when its acetylation was lower. Conversely, ASS1-Flag showed lower activity at 24 and 48 hr after synchronization, when its acetylation was higher (Figures 5F and S6F). Although circadian rhythms of metabolite content were difficult to detect in cultured cells, ureagenesis was monitored as an increasing amount of urea within a given period treated with alanine, the exogenous nitrogen source (Soria et al., 2013). The production rate of urea was higher at 36 hr after DXM synchronization in HL-7702 hepatocytes, compared with 24 hr after DXM (Figure 5G). In CLOCK knockdown cells with two independent siRNAs, urea production did not exhibit significant oscillation between 24 and 36 hr after DXM, both of which were similar to the rate at 36 hr after DXM in control HL-7702 cells (Figure 5G). The urea content (Figure 5H) and relative arginine abundance (Figure S6G) were monitored in mouse liver sampled from ZT0 to ZT24 with a 4-hr interval. Urea content oscillated, while arginine abundance also displayed mild oscillation. The peaks of either urea or arginine were detected at ZT0 and ZT24, the time points corresponding to troughs of ASS1 acetylation cycle in mouse liver. Evidenced by our findings on the oscillation of ASS1 acetylation, enzymatic activity, and metabolites, we propose that arginine biosynthesis and urea cycle are rhythmically gated by CLOCK-dependent acetylation of ASS1.

CLOCK Is a Rhythmic Acetyl-Transferase for NDUFA9 and IMPDH2

Our study has unraveled ASS1 as an acetylation substrate of CLOCK to modulate the rhythmicity of arginine and urea metabolism. To expand our understanding of CLOCK in metabolic regulation, we employed LC-MS/MS to identify CLOCK-interacting proteins. As expected, BMAL1 was among the top CLOCK-interacting proteins detected (Figure 6A). We also observed several metabolic enzymes, including NDUFA9 and IMPDH2 as putative CLOCK-interacting proteins. Interestingly, both NDUFA9 and IMPDH2 exhibited circadian acetylation in U2OS cells after DXM synchronization (Figure S7A), indicating that they are additional rhythmic substrates of CLOCK acetylation. The interaction between NDUFA9 or IMPDH2 and CLOCK was verified by co-immunoprecipitation of proteins ectopically expressed in HEK293T cells (Figure 6B).

We found that Flag-tagged NDUFA9 and IMPDH2 were acetylated in WT U2OS cells (Figure 6C). Moreover, NDUFA9 acetylation was completely suppressed in CLOCK KO#1/KO#2 cells while IMPDH2 acetylation was also significantly attenuated, indicating that CLOCK regulates the acetylation of both NDUFA9 and IMPDH2. Acetylation of IMPDH2 by CLOCK was further examined by in vitro assay. IMPDH2 expressed and purified from *E. coli* was acetylated by CLOCKΔN in a dose-dependent manner (Figures 6D and S7B), while the specificity of such acetylation assay was confirmed by the inability of CLOCKΔN to acetylate ALDH1A1 (Figure S7C), an enzyme that is known to be acetylated (Zhao et al., 2014). Similar to ASS1, much lower endogenous CLOCK was detected in immunoprecipitate of Flag-tagged IMPDH2 at 36 hr after DXM, which is compared with 24 and 48 hr in U2OS cells (Figure 6E). The correlation between CLOCK association and acetylation implies that rhythmic binding of CLOCK to IMPDH2 may attribute to the rhythmic change of IMPDH2 acetylation. IMPDH1/IMPDH12 catalyzes the conversion of inosine 5′-phosphate (IMP) to xanthosine 5′-phosphate (XMP), the first and rate-limiting step of guanine nucleotide biosynthesis. Notably, our metabolic profiling data for CLOCK KO#1 U2OS cells showed

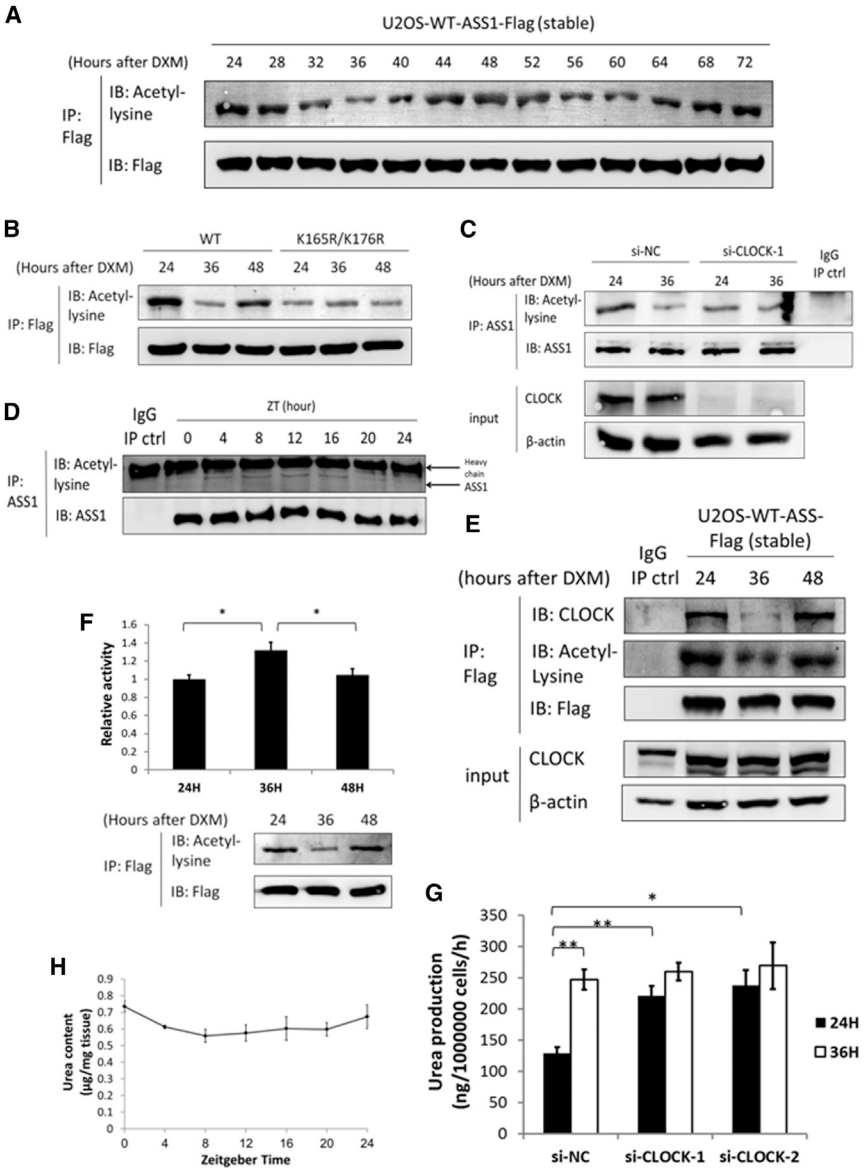

Figure 5. Rhythmic Acetylation of ASS1 and Circadian Cycle of Ureagenesis

(A) Acetylation of ectopically expressed ASS1 oscillates in U2OS cells. ASS1-Flag was stably expressed in WT U2OS cells. Dexamethasone (DXM) treatment for 24 hr was used to synchronize U2OS cells. Cells were harvested from 24 to 72 hr with 4-hr intervals, and ASS1-Flag was immunoprecipitated with anti-Flag antibody. Acetylation of the precipitated ASS1-Flag was determined by western blotting with anti-acetyl-lysine antibody.

(B) Acetylation of ectopically expressed WT, but not the K165R/K176R mutant ASS1, oscillates in U2OS cells. Flag-tagged WT or K165R/K176R mutant ASS1 was transfected in WT U2OS cells and immunoprecipitated by anti-Flag in the cell lysates sampled at 24, 36, and 48 hr after synchronization by DXM. Acetylation was determined by western blotting with anti-acetyl-lysine antibody in immunoprecipitate.

(C) CLOCK knockdown decreases acetylation of endogenous ASS1 in HL-7702 hepatocytes. The immortalized HL-7702 hepatocytes were transfected with negative control (NC) or CLOCK-targeting siRNA. Endogenous ASS1 was immunoprecipitated by ASS1 antibody from cells sampled at 24 and 36 hr after synchronization by DXM. Acetylation was determined by western blotting with anti-acetyl-lysine antibody in immunoprecipitate.

(D) Acetylation of endogenous ASS1 oscillates in mouse livers. Endogenous ASS1 was immunoprecipitated by ASS1 antibody from WT mouse livers sampled from ZT0 to ZT24 with 4-hr intervals. Livers from three mice at each sampling time point were combined prior to immunoprecipitation. Acetylation was determined by western blotting with anti-acetyl-lysine antibody in immunoprecipitate. Note, both the IgG heavy chain and ASS1 in immunoprecipitates are indicated by arrows.

(E) CLOCK rhythmically associates with ASS1 in U2OS cells. ASS1-Flag was immunoprecipitated by anti-Flag antibody from WT U2OS cells harboring stable transgene of ASS1-Flag. Samples were collected at 24, 36, and 48 hr after synchronization by DXM. Co-immunoprecipitation of endogenous CLOCK was detected by western blotting. Acetylation of ASS1-Flag was determined by western blotting with anti-acetyl-lysine antibody.

(F) Activity of ectopically expressed ASS1 oscillates in U2OS cells. ASS1-Flag was transfected in WT U2OS cells and immunoprecipitated by anti-Flag from these cells sampled at 24, 36, and 48 hr after synchronization by DXM. Enzymatic activity of the immunoprecipitated ASS1 was monitored by di-phosphate release from the argininosuccinate synthesis reaction. Top: relative enzymatic activity, n = 5 for each bar. Bottom: western blotting detection of acetylation and protein levels of ASS1-Flag that was used in enzymatic activity assay.

(G) Urea production oscillates in control, but not CLOCK knockdown HL-7702 hepatocytes. HL-7702 cells were transfected with siRNA negative control (NC) or two independent siRNAs targeting CLOCK. Alanine (10 mM) was added to stimulate ureagenesis at 24 and 36 hr after synchronization by DXM. Five hours after alanine treatment, urea production was calculated as net increase of urea monitored by GC-MS. n = 3 for each bar.

(H) Urea content oscillates in mice livers. WT mouse livers were sampled from ZT0 to ZT24 with 4-hr intervals. The total metabolites were extracted and urea content was monitored by GC-MS with commercial urea chemical as a standard. n = 4 for each ZT time point.

Data are graphed as the mean ± SEM, *p < 0.05, **p < 0.01. See also Figure S6.

that guanosine and guanosine diphosphate (GDP) were both elevated in CLOCK KO cells (Table S1; guanosine, fold change = 2.73, p = 0.008; GDP, fold change = 2.89, p = 0.021). Together, our data suggest that CLOCK regulates IMPDH2 enzymatic activity by acetylation to influence guanine nucleotide metabolism.

DISCUSSION

Cycling expression of metabolic enzymes at both mRNA and protein levels is of crucial importance for the metabolic rhythmicity. In the present study, we identified certain metabolic enzymes (ASS1, IMPDH2, and NDUFA9) to be direct

A

Protein names	Gene names	LFQ intensity	LFQ intensity ctrl
Aryl hydrocarbon receptor nuclear translocator-like protein 1	ARNTL (BMAL1)	29609000	0
Circadian locomoter output cycles protein kaput	CLOCK	27610000	0
Inosine-5-monophosphate dehydrogenase 2	**IMPDH2**	**3060800**	**0**
Aryl hydrocarbon receptor nuclear translocator-like protein 2	ARNTL2 (BMAL2)	2162600	0
NADH dehydrogenase [ubiquinone] 1 alpha subcomplex subunit 9, mitochondrial	**NDUFA9**	**652760**	**0**
Thioredoxin	**TXN**	**537060**	**0**
7-dehydrocholesterol reductase	**DHCR7**	**130580**	**0**

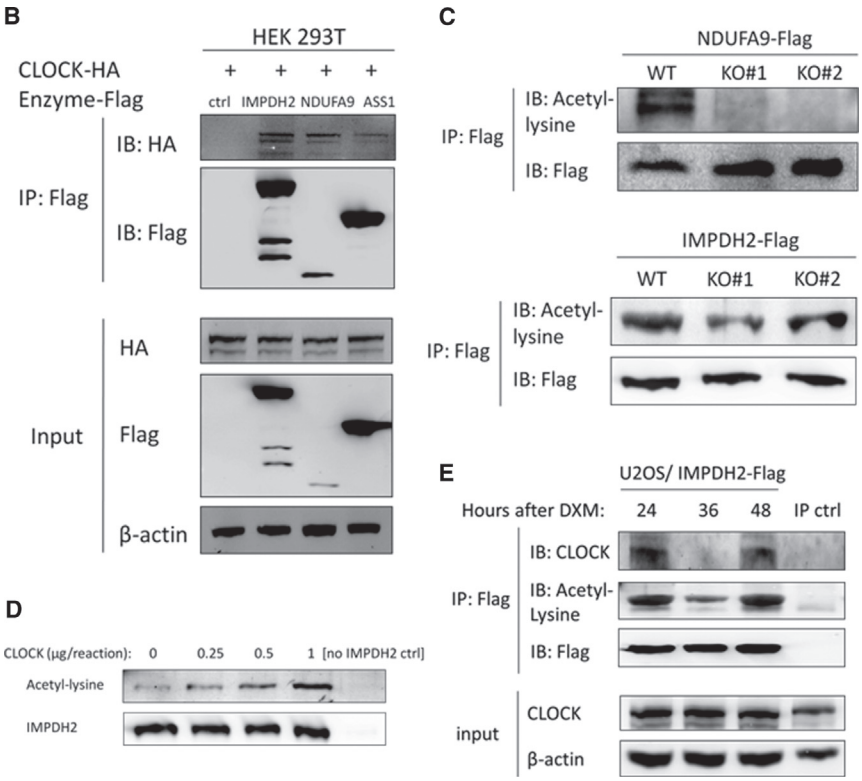

Figure 6. NDUFA9 and IMPDH2 Are Acetylation Substrates of CLOCK

(A) Metabolic enzymes are identified as CLOCK interacting proteins. Ectopically expressed SBP-tagged CLOCK in WT U2OS cells was purified with streptavidin beads and the co-purified proteins were trypsin-digested and analyzed by high-performance liquid chromatography (HPLC)-MS/MS. Besides the known CLOCK partner BMAL1, metabolic enzymes, which are highlighted, are among the top CLOCK interacting proteins.

(B) Ectopically expressed CLOCK binds to ectopically expressed NDUFA9 or IMPDH2. Flag-tagged NDUFA9 or IMPDH2 was transfected in HEK293T cells and immunoprecipitated by anti-Flag antibody, taking ASS1-Flag and empty Flag as positive and negative control, respectively. HA-tagged CLOCK was co-transfected and its co-immunoprecipitation was detected by western blotting with anti-HA antibody in the Flag immunoprecipitate.

(C) Acetylation of ectopically expressed NDUFA9 or IMPDH2 is declined in CLOCK KO U2OS cells. Flag-tagged NDUFA9 (top panels) or IMPDH2 (bottom panels) was transfected into WT, CLOCK KO#1, and KO#2 U2OS cells. Acetylation was determined by western blotting with anti-acetyl-lysine antibody in immunoprecipitate of Flag.

(D) CLOCKΔN acetylates IMPDH2 in a dose-dependent manner in vitro. The *E. coli*-expressed and purified recombinant IMPDH2 was incubated in vitro with acetyl-CoA and increasing doses of purified recombinant CLOCKΔN. Acetylation of IMPDH2 was determined by western blotting with anti-acetyl-lysine antibody.

(E) CLOCK rhythmically associates with IMPDH2 in U2OS cells. Transfected IMPDH2-Flag was immunoprecipitated by anti-Flag antibody from WT U2OS cells sampled at 24, 36, and 48 hr after synchronization by DXM. Co-immunoprecipitation of endogenous CLOCK was detected by western blotting. Acetylation of IMPDH2-Flag was determined by western blotting with anti-acetyl-lysine antibody.

See also Figure S7.

acetylation substrates of CLOCK whose acetyl-transferase activity is as important as its transcription activity in circadian control. With the help of BMAL1, CLOCK rhythmically interacts with cytosolic ASS1 to acetylate K165 and K176, leading to enzymatic inhibition of ASS1 as well as the circadian oscillation of arginine biosynthesis and subsequent ureagenesis (Figure 7). The rhythmic interaction with and acetylation by CLOCK were also observed for IMPDH2, an enzyme critical in guanine nucleotide biosynthesis, indicating a broad role of CLOCK in circadian regulation of metabolism at the post-translational level.

Acetylation Governs Circadian Rhythms of Metabolic Enzyme Activity

The circadian clock governs not only the abundance of mRNA and protein, but also the activity of metabolic enzymes. Given the effect of acetylation on a broad range of metabolic enzymes (Guan and Xiong, 2011), acetylation might represent a global strategy in rhythmic regulation of metabolic enzymes at post-translational level, as implied by a proteomic investigation (Masri et al., 2013). This report provides direct evidence that CLOCK modulates metabolism circadian by acetylating metabolic enzymes.

Previous studies have revealed that post-translational modifications to central clock proteins (like PER and CRY) are indispensable to maintain normal circadian clocks (Nawathean et al., 2007; Öllinger et al., 2014; Saez et al., 2011; Vielhaber et al., 2001). Prompted by the findings from metabolic profiling in U2OS cells, we discovered that rhythmic CLOCK-dependent acetylation of ASS1 at K165 and K176 residues contributes to the temporal gating of arginine biosynthesis and ureagenesis. We also identified IMPDH2 and NDUFA9 to be potential substrates of rhythmic CLOCK-induced acetylation. These observations suggest that acetylation of metabolic enzymes by CLOCK plays a critical role in the circadian regulation of metabolic pathways.

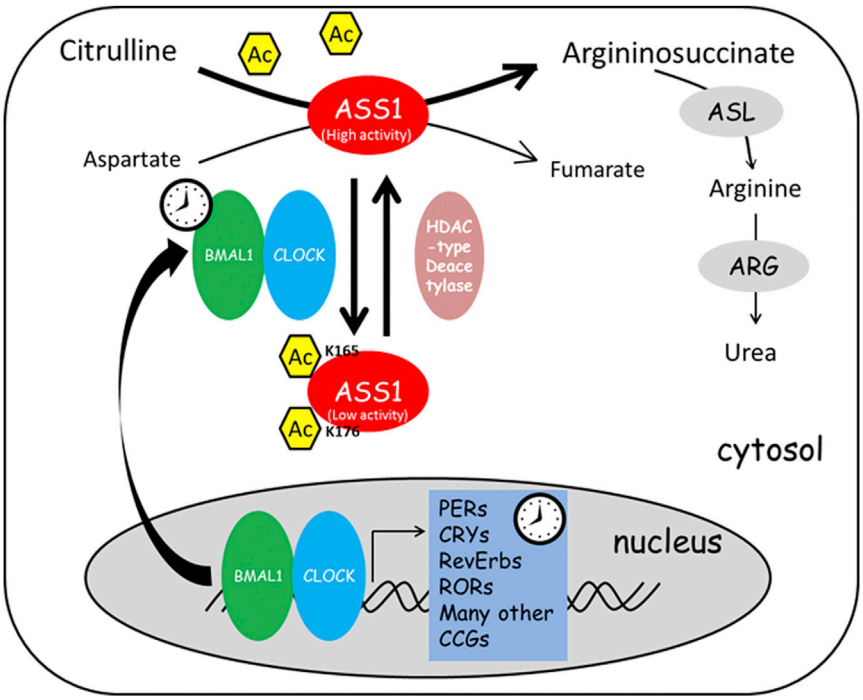

Figure 7. A Proposed Model for CLOCK in Regulation of Arginine Biosynthesis and Ureagenesis via ASS1 Acetylation

A schematic model depicting the CLOCK-regulated acetylation switch of ASS1 involved in arginine biosynthesis and ureagenesis. Acetylation at K165 and K176 by CLOCK inhibits the enzymatic activity of ASS1. CLOCK acts as a rhythmic acetyl-transferase, a function distinct from its canonical transcription factor, toward metabolic enzymes in circadian regulation.

CLOCK Acts as a Rhythmic Acetyl-Transferase for Metabolic Enzymes

The role of acetylation in rhythmic gating of metabolic enzymes was previously supported (Peek et al., 2013; Sahar et al., 2014), where Sirtuins were considered as important regulators of acetylation cycle. Activity of all Sirtuin-family deacetylases rely on NAD^+, whose salvage biosynthesis pathway cycles due to rhythmic expression of nicotinamide phosphoribosyl-transferase (NAMPT), a direct transcription target of CLOCK/BMAL1 (Nakahata et al., 2009; Ramsey et al., 2009), hence reflecting a loop of circadian clock control on protein acetylation. In contrast, acetyl-transferases for metabolic enzymes involved in circadian regulation have not been revealed in previous studies.

CLOCK has histone acetyl-transferase activity (Doi et al., 2006), and its acetylation targets include certain non-histone proteins, such as its binding partner, BMAL1 (Hirayama et al., 2007). Our study demonstrates that CLOCK is responsible for rhythmic ASS1 acetylation, which negatively regulates ASS1 activity. It is worth noting that BMAL1 is important for the proper ASS1 acetylation by CLOCK in the cell, indicating that BMAL1 is also directly involved in posttranscriptional regulation of metabolic enzymes. We further showed that HDACs, but not Sirtuins, are responsible for ASS1 deacetylation. Notably, it has been reported that SIRT1 associates with CLOCK/BMAL1 and promotes deacetylation of H3 and BMAL1 (Nakahata et al., 2008). HDACs are considered to be non-rhythmic whereas Sirtuin activity can be rhythmic due to fluctuation of its co-factor NAD (Figures S2D and S2E). Hence, the oscillation of ASS1 acetylation is likely to be controlled by the CLOCK acetyl-transferase, but not by deacetylase.

The regulatory role of CLOCK in ASS1 acetylation cycle is further supported by the rhythmic interaction between CLOCK and ASS1 in both DXM-synchronized U2OS cells and mouse liver. Furthermore, we also observed that CLOCK controls the acetylation of NDUFA9 and IMPDH2, and the association of CLOCK with IMPDH2 is rhythmic, suggesting a potential broad role of CLOCK in the circadian regulation of metabolism. Although CLOCK distributes in both cytosol and nucleus, the distribution of CLOCK in these two compartments is not altered during circadian cycles. Therefore, future study is required to reveal the molecular basis for the rhythmic interaction between CLOCK and its metabolic substrates.

CLOCK in the Temporal Control of Arginine Biosynthesis and Ureagenesis

The rhythmic acetylation leads to cyclic inhibition of ASS1. This observation is consistent with the oscillation of arginine and urea biosynthesis in both DXM-synchronized U2OS cells and mouse liver. Moreover, the acceleration of arginine and urea production takes place at the time when ASS1 is predominantly deacetylated, the condition of high ASS1 activity. The rhythmic inactivation of ASS1 regulated by CLOCK is further supported by our analysis of published datasets (Circadiomics) (Patel et al., 2012). In mouse liver circadian proteome and metabolome, there is an anti-phasing relationship between urea/arginine levels and CLOCK/BMAL1 protein abundance (Patel et al., 2012).

The circadian clock has a broad impact on most metabolic pathways. Urea cycle is the major pathway engaged in disposal of excess nitrogen. Arginine metabolism is an integral step in urea cycle, as ornithine produced from arginine hydrolization is further converted to citrulline by OTC to re-start the cycle. A previous study revealed that OTC in mitochondria is controlled by SIRT3 deacetylation in a rhythmic manner (Peek et al., 2013). Here, we show that ASS1 activity is suppressed by CLOCK via direct acetylation in a rhythmic manner, which drives the temporal variation of arginine biosynthesis and subsequent ureagenesis. Therefore, multiple mechanisms (SIRT3-dependent deacetylation of OTC and CLOCK-dependent acetylation of ASS1) are utilized to ensure the proper circadian nature of urea cycle.

In summary, our findings of rhythmic acetylation of ASS1, NDUFA9, and IMPDH2 by CLOCK demonstrate that CLOCK,

the key component of central clock circuitry, could act as an acetyl-transferase for metabolic enzymes with functional significance, hence expanding our knowledge on both acetylation control for metabolic enzymes and temporal fluctuation of metabolic function regulated by the central circadian machinery, CLOCK and BMAL1. In conjunction with the identification of multiple metabolic enzymes as substrates of CLOCK acetylation, this study also raises a new possibility for therapeutics to combat metabolic impairment caused by aberrant circadian clock, which is becoming a risk factor to human health in this modern society with a much more complex lifestyle than before.

STAR★METHODS

Detailed methods are provided in the online version of this paper and include the following:

- KEY RESOURCES TABLE
- CONTACT FOR REAGENT AND RESOURCE SHARING
- EXPERIMENTAL MODEL AND SUBJECT DETAILS
  - Cell lines
  - Animal sample collection
- METHOD DETAILS
  - Generation of clock and ass1 knock-out U2OS cell lines
  - Generation of stable transfection cell pools
  - RNA interference
  - RNA isolation and quantitative RT-PCR
  - Immunoprecipitation, elution and western blotting
  - Protein expression and purification
  - Protein Quantification
  - GC-MS analysis for urea
  - LC-MS analysis for metabolites
  - LC-MS/MS analysis for acetylation sites in ASS1
  - LC-MS/MS analysis for CLOCK-interacting proteins
  - In vitro acetylation assay
  - ASS1 activity assay
  - Cell proliferation assay
- QUANTIFICATION AND STATISTICAL ANALYSIS

SUPPLEMENTAL INFORMATION

Supplemental Information includes seven figures and two tables and can be found with this article online at https://doi.org/10.1016/j.molcel.2017.09.008.

AUTHOR CONTRIBUTIONS

R.L., Y. Xiong, and K.-L.G. conceived and designed the experiments. R.L., Y.M., and H.Z. performed the experiments. R.L., Y.M., Y. Xu, Y. Xiong, and K.-L.G. analyzed the data. Z.Q., P.X., Y. Xu, H.Z., and Z.-J.Z. contributed reagents, materials, and analysis tools. R.L. and K.-L.G. wrote the paper. R.L., Y. Xiong, and K.-L.G. conceived, initiated, and supervised the project.

ACKNOWLEDGMENTS

The authors would like to thank members of the Fudan-MCB lab for technical assistance, helpful discussions, and comments regarding this manuscript. We thank Dr. Jun Yao at the Institute of Biomedical Sciences, Fudan University for assistance on LC-MS/MS analysis of CLOCK-interacting proteins, Dr. Lei Song at the Beijing Proteome Research Center for assistance on LC-MS/MS analysis of ASS1 acetylation residues, and Shanghai Applied Protein Technology for assistance on metabolomic LC-MS/MS analysis. This work was supported by the MOST (Ministry of Science and Technology of China) 973 (2015CB910401 and 2016YFA0501801 to Y. Xiong), the NSFC (Natural Science Foundation of China) (31500953 to R.L.), and the CPSF (China Postdoctoral Science Foundation) (142062 to R.L.).

Received: April 3, 2017
Revised: July 24, 2017
Accepted: September 6, 2017
Published: October 5, 2017

REFERENCES

Altman, B.J., Hsieh, A.L., Sengupta, A., Krishnanaiah, S.Y., Stine, Z.E., Walton, Z.E., Gouw, A.M., Venkataraman, A., Li, B., Goraksha-Hicks, P., et al. (2015). MYC disrupts the circadian clock and metabolism in cancer cells. Cell Metab. *22*, 1009–1019.

Bunger, M.K., Wilsbacher, L.D., Moran, S.M., Clendenin, C., Radcliffe, L.A., Hogenesch, J.B., Simon, M.C., Takahashi, J.S., and Bradfield, C.A. (2000). Mop3 is an essential component of the master circadian pacemaker in mammals. Cell *103*, 1009–1017.

Chong, S.Y., Ptáček, L.J., and Fu, Y.H. (2012). Genetic insights on sleep schedules: this time, it's PERsonal. Trends Genet. *28*, 598–605.

de Boor, S., Knyphausen, P., Kuhlmann, N., Wroblowski, S., Brenig, J., Scislowski, L., Baldus, L., Nolte, H., Krüger, M., and Lammers, M. (2015). Small GTP-binding protein Ran is regulated by posttranslational lysine acetylation. Proc. Natl. Acad. Sci. USA *112*, E3679–E3688.

Doi, M., Hirayama, J., and Sassone-Corsi, P. (2006). Circadian regulator CLOCK is a histone acetyltransferase. Cell *125*, 497–508.

Feng, D., and Lazar, M.A. (2012). Clocks, metabolism, and the epigenome. Mol. Cell *47*, 158–167.

Grozinger, C.M., Chao, E.D., Blackwell, H.E., Moazed, D., and Schreiber, S.L. (2001). Identification of a class of small molecule inhibitors of the sirtuin family of NAD-dependent deacetylases by phenotypic screening. J. Biol. Chem. *276*, 38837–38843.

Guan, K.L., and Xiong, Y. (2011). Regulation of intermediary metabolism by protein acetylation. Trends Biochem. Sci. *36*, 108–116.

Guerreiro, J.R., Lameu, C., Oliveira, E.F., Klitzke, C.F., Melo, R.L., Linares, E., Augusto, O., Fox, J.W., Lebrun, I., Serrano, S.M., and Camargo, A.C. (2009). Argininosuccinate synthetase is a functional target for a snake venom anti-hypertensive peptide: role in arginine and nitric oxide production. J. Biol. Chem. *284*, 20022–20033.

Hirayama, J., Sahar, S., Grimaldi, B., Tamaru, T., Takamatsu, K., Nakahata, Y., and Sassone-Corsi, P. (2007). CLOCK-mediated acetylation of BMAL1 controls circadian function. Nature *450*, 1086–1090.

Huang, N., Chelliah, Y., Shan, Y., Taylor, C.A., Yoo, S.H., Partch, C., Green, C.B., Zhang, H., and Takahashi, J.S. (2012). Crystal structure of the heterodimeric CLOCK:BMAL1 transcriptional activator complex. Science *337*, 189–194.

Karlberg, T., Collins, R., van den Berg, S., Flores, A., Hammarström, M., Högbom, M., Holmberg Schiavone, L., and Uppenberg, J. (2008). Structure of human argininosuccinate synthetase. Acta Crystallogr. D Biol. Crystallogr. *64*, 279–286.

Kettner, N.M., Voicu, H., Finegold, M.J., Coarfa, C., Sreekumar, A., Putluri, N., Katchy, C.A., Lee, C., Moore, D.D., and Fu, L. (2016). Circadian homeostasis of liver metabolism suppresses hepatocarcinogenesis. Cancer Cell *30*, 909–924.

Lamia, K.A., Storch, K.F., and Weitz, C.J. (2008). Physiological significance of a peripheral tissue circadian clock. Proc. Natl. Acad. Sci. USA *105*, 15172–15177.

Masri, S., Patel, V.R., Eckel-Mahan, K.L., Peleg, S., Forne, I., Ladurner, A.G., Baldi, P., Imhof, A., and Sassone-Corsi, P. (2013). Circadian acetylome reveals regulation of mitochondrial metabolic pathways. Proc. Natl. Acad. Sci. USA *110*, 3339–3344.

Nakahata, Y., Kaluzova, M., Grimaldi, B., Sahar, S., Hirayama, J., Chen, D., Guarente, L.P., and Sassone-Corsi, P. (2008). The NAD+-dependent deacetylase SIRT1 modulates CLOCK-mediated chromatin remodeling and circadian control. Cell *134*, 329–340.

Nakahata, Y., Sahar, S., Astarita, G., Kaluzova, M., and Sassone-Corsi, P. (2009). Circadian control of the NAD+ salvage pathway by CLOCK-SIRT1. Science *324*, 654–657.

Nawathean, P., Stoleru, D., and Rosbash, M. (2007). A small conserved domain of Drosophila PERIOD is important for circadian phosphorylation, nuclear localization, and transcriptional repressor activity. Mol. Cell. Biol. *27*, 5002–5013.

Öllinger, R., Korge, S., Korte, T., Koller, B., Herrmann, A., and Kramer, A. (2014). Dynamics of the circadian clock protein PERIOD2 in living cells. J. Cell Sci. *127*, 4322–4328.

Partch, C.L., Green, C.B., and Takahashi, J.S. (2014). Molecular architecture of the mammalian circadian clock. Trends Cell Biol. *24*, 90–99.

Patel, V.R., Eckel-Mahan, K., Sassone-Corsi, P., and Baldi, P. (2012). CircadiOmics: integrating circadian genomics, transcriptomics, proteomics and metabolomics. Nat. Methods *9*, 772–773.

Peek, C.B., Affinati, A.H., Ramsey, K.M., Kuo, H.Y., Yu, W., Sena, L.A., Ilkayeva, O., Marcheva, B., Kobayashi, Y., Omura, C., et al. (2013). Circadian clock NAD+ cycle drives mitochondrial oxidative metabolism in mice. Science *342*, 1243417.

Ramsey, K.M., Yoshino, J., Brace, C.S., Abrassart, D., Kobayashi, Y., Marcheva, B., Hong, H.K., Chong, J.L., Buhr, E.D., Lee, C., et al. (2009). Circadian clock feedback cycle through NAMPT-mediated NAD+ biosynthesis. Science *324*, 651–654.

Ran, F.A., Hsu, P.D., Wright, J., Agarwala, V., Scott, D.A., and Zhang, F. (2013). Genome engineering using the CRISPR-Cas9 system. Nat. Protoc. *8*, 2281–2308.

Reddy, A.B., and O'Neill, J.S. (2010). Healthy clocks, healthy body, healthy mind. Trends Cell Biol. *20*, 36–44.

Rudic, R.D., McNamara, P., Curtis, A.M., Boston, R.C., Panda, S., Hogenesch, J.B., and Fitzgerald, G.A. (2004). BMAL1 and CLOCK, two essential components of the circadian clock, are involved in glucose homeostasis. PLoS Biol. *2*, e377.

Saez, L., Derasmo, M., Meyer, P., Stieglitz, J., and Young, M.W. (2011). A key temporal delay in the circadian cycle of Drosophila is mediated by a nuclear localization signal in the timeless protein. Genetics *188*, 591–600.

Sahar, S., Masubuchi, S., Eckel-Mahan, K., Vollmer, S., Galla, L., Ceglia, N., Masri, S., Barth, T.K., Grimaldi, B., Oluyemi, O., et al. (2014). Circadian control of fatty acid elongation by SIRT1 protein-mediated deacetylation of acetyl-coenzyme A synthetase 1. J. Biol. Chem. *289*, 6091–6097.

Shimba, S., Ogawa, T., Hitosugi, S., Ichihashi, Y., Nakadaira, Y., Kobayashi, M., Tezuka, M., Kosuge, Y., Ishige, K., Ito, Y., et al. (2011). Deficient of a clock gene, brain and muscle Arnt-like protein-1 (BMAL1), induces dyslipidemia and ectopic fat formation. PLoS ONE *6*, e25231.

Soria, L.R., Marrone, J., Calamita, G., and Marinelli, R.A. (2013). Ammonia detoxification via ureagenesis in rat hepatocytes involves mitochondrial aquaporin-8 channels. Hepatology *57*, 2061–2071.

Turek, F.W., Joshu, C., Kohsaka, A., Lin, E., Ivanova, G., McDearmon, E., Laposky, A., Losee-Olson, S., Easton, A., Jensen, D.R., et al. (2005). Obesity and metabolic syndrome in circadian Clock mutant mice. Science *308*, 1043–1045.

Vielhaber, E.L., Duricka, D., Ullman, K.S., and Virshup, D.M. (2001). Nuclear export of mammalian PERIOD proteins. J. Biol. Chem. *276*, 45921–45927.

Xu, Y., Toh, K.L., Jones, C.R., Shin, J.Y., Fu, Y.H., and Ptácek, L.J. (2007). Modeling of a human circadian mutation yields insights into clock regulation by PER2. Cell *128*, 59–70.

Xu, K., Zheng, X., and Sehgal, A. (2008). Regulation of feeding and metabolism by neuronal and peripheral clocks in Drosophila. Cell Metab. *8*, 289–300.

Yoshida, M., Kijima, M., Akita, M., and Beppu, T. (1990). Potent and specific inhibition of mammalian histone deacetylase both in vivo and in vitro by trichostatin A. J. Biol. Chem. *265*, 17174–17179.

Zhao, S., Xu, W., Jiang, W., Yu, W., Lin, Y., Zhang, T., Yao, J., Zhou, L., Zeng, Y., Li, H., et al. (2010). Regulation of cellular metabolism by protein lysine acetylation. Science *327*, 1000–1004.

Zhao, D., Mo, Y., Li, M.T., Zou, S.W., Cheng, Z.L., Sun, Y.P., Xiong, Y., Guan, K.L., and Lei, Q.Y. (2014). NOTCH-induced aldehyde dehydrogenase 1A1 deacetylation promotes breast cancer stem cells. J. Clin. Invest. *124*, 5453–5465.

STAR★METHODS

KEY RESOURCES TABLE

REAGENT or RESOURCE	SOURCE	IDENTIFIER
Antibodies		
Anti-ASL	Abcam	Ab201025
Anti-IMPDH2	Abcam	Ab131158; RRID: AB_11156264
Anti-RevErb-alpha	Abcam	Ab174309
Anti-Histone H3	Cell Signaling	#9715; RRID: AB_331563
Anti-acetyl-lysine	Cell Signaling	#9681; RRID: AB_331799
Anti-Lamin A/C	GenScript	A01455; RRID: AB_1720882
Anti-actin	GenScript	A00702; RRID: AB_914102
Horseradish peroxidase-labeled goat anti-rabbit IgG	GenScript	A00098; RRID: AB_1968815
Anti-tubulin	NeoMarkers	#581P
Anti-ASS1 (for IP and WB)	ProteinTech	16210-1-AP; RRID: AB_2060466
Anti-BMAL1	ProteinTech	14268-1-AP
Anti-HA	Santa Cruz	Sc-7392; RRID: AB_627809
Anti-ASS1 (for WB)	Santa Cruz	Sc-46066; RRID: AB_2060477
Anti-CLOCK	Santa Cruz	Sc-25316
Anti-ALDH1A1	Santa Cruz	Sc-374149; RRID: AB_10917910
Anti-FLAG	Sigma-Aldrich	F7425; RRID: AB_439687
Horseradish peroxidase-labeled rabbit anti-mouse IgG	SouthernBiotech	6170-05
Anti-Period 2	In house (Xu et al., 2007)	N/A
Bacterial and Virus Strains		
DH5alpha *Escherichia coli*	Tiangen Biotech	CB101
BL21 *Escherichia coli*	Tiangen Biotech	CB105
Biological Samples		
Mouse liver samples	Ying Xu lab	N/A
Chemicals, Peptides, and Recombinant Proteins		
Dexamethasone	Sigma-Aldrich	D1756
L-citrulline	Sigma-Aldrich	C7629
L-aspartic acid	Sigma-Aldrich	A5474
adenosine 5′-triphosphate (ATP) magnesium salt	Sigma-Aldrich	A7699
Acetyl-CoA sodium salt	Sigma-Aldrich	A2056
Beta-Nicotinamide adenine dinucleotide 2′-phosphate reduced tetrasodium salt	Sigma-Aldrich	N9660
Trichostatin A	Cell Signaling	#9950
sirtinol	Selleck	S2804
Histone H3	Abcam	Ab198757
pyrophosphatase	New England Biolabs	M0296
CLOCKΔN (His-tagged)	In this paper	N/A
WT ASS1 (His-tagged)	In this paper	N/A
K165R/K176R ASS1 (His-tagged)	In this paper	N/A
K165Q/K176Q ASS1 (His-tagged)	In this paper	N/A
IMPDH2 (His-tagged)	In this paper	N/A
ALDH1A1 (His-tagged)	In this paper	N/A

(*Continued on next page*)

Continued

REAGENT or RESOURCE	SOURCE	IDENTIFIER
Critical Commercial Assays		
Malachite Green Phosphate Assay Kit	Cayman Chemical	#10009325
Experimental Models: Cell Lines		
U2OS	ATCC	HTB-96
U2OS with clock knock-out #1	In this paper	N/A
U2OS with clock knock-out #2	In this paper	N/A
U2OS with ass1 knock-out	In this paper	N/A
HEK293T	ATCC	CRL-3216
HL-7702	Cell bank, Chinese Academy of Sciences	GNHu-6
Oligonucleotides		
sgRNA targeting clock: 5′-CTAGTGAAATTCGACAGGAC-3′	In this paper	N/A
sgRNA targeting ass1: 5′-TATGTGTCCCACGGCGCCAC-3′	In this paper	N/A
siRNA targeting clock #1: 5′- GCTGGAAAGTGACTCATTA −3′	In this paper	N/A
siRNA targeting clock #2: 5′- GGAAATGTGTACTGTTGAA −3′	In this paper	N/A
siRNA targeting bmal1 #1: 5′- TCGCAATTGGACGACTGCATTCTCA −3′	In this paper	N/A
siRNA targeting bmal1 #2: 5′- TGACTACCTGCATCCTAAAGATATT −3′	In this paper	N/A
siRNA negative control: 5′- TTCTCCGAACGTGTCACGT −3′	In this paper	N/A
Primers for RT-PCR detection of ass1, asl, per2, gapdh, see Table S2	In this paper	N/A
Recombinant DNA		
pcDNA3.1b-CLOCK-HA or Myc-His	In this paper	N/A
pcDNA3.1b-BMAL1-HA	In this paper	N/A
pcDNA3.1b-ASS1 (WT or K165R/K176R)-Flag	In this paper	N/A
pcDNA3.1b-IMPDH2-Flag	In this paper	N/A
pcDNA3.1b-NDUFA9-Flag	In this paper	N/A
pcDNA3.1b-ASL-Flag	In this paper	N/A
pBABE-CLOCK (WT or mutA/B)	In this paper	N/A
pBABE-ASS1-Flag	In this paper	N/A
pBABE-SBP-CLOCK	In this paper	N/A
pET21b-CLOCKΔN	In this paper	N/A
pET21b-ASS1 (WT, K165R/K176R, K165Q/K176Q)	In this paper	N/A
pET21b-IMPDH2	In this paper	N/A
pET21b-ALDH1A1	In this paper	N/A
px458 or 459-targeting clock	In this paper	N/A
px458 or 459-targeting ass1	In this paper	N/A

CONTACT FOR REAGENT AND RESOURCE SHARING

Further information and requests for resources and reagents should be directed to and will be fulfilled by the Lead Contact, Ran Lin (rlin@fudan.edu.cn).

EXPERIMENTAL MODEL AND SUBJECT DETAILS

Cell lines

HEK293T, U2OS and HL-7702 cells were cultured in Dulbecco's modified Eagle's medium (DMEM, GIBCO) supplemented with fetal bovine serum (FBS, GIBCO, HEK293T for 5%, U2OS and HL-7702 for 10%) and antibiotics (100units/ml penicillin and 100 μg/ml streptomycin), in 5% CO2 atmosphere at 37°C. U2OS and HL-7702 cells were synchronized by 2 hr treatment of DXM (100nM) and sampled at various time points after DXM withdrawal.

Animal sample collection

Male (8 weeks old) WT or bmal1 whole body knock-out mice with C57BL/6J background (Bunger et al., 2000) were entrained to a 12h/12h light/dark cycle for at least seven days before tissue collection. Livers were taken from the Zeitgeber times (ZT) ZT-0 to ZT-24 with 4 hr interval, where ZT-12 corresponds to the onset of subjective night.

All animal studies were carried out in an Association for Assessment and Accreditation of Laboratory Animal Care internationally accredited specific pathogen-free animal facility, and all animal protocols were approved by the Animal Care and Use Committee of the Model Animal Research Center, the host for the National Resource Center for Mutant Mice in China.

METHOD DETAILS

Generation of clock and ass1 knock-out U2OS cell lines

Generation of knock-out cells was described elsewhere (Ran et al., 2013). The 20-nucleotides guide sequence targeting the third exon within Coding sequence (CDS) of human clock gene was listed in the Key Resources Table, and the guide sequence targeting the third exon within CDS of human ass1 gene was listed in the Key Resources Table. Guide sequences were cloned into a bicistronic expression vector (pX458) containing human codon-optimized Cas9 and the RNA components, as well as egfp gene for screening. Single clones of U2OS cells expanded after transfection and EGFP sorting were detected by both western blotting for whole cell lysate and Sanger sequencing for genomic DNA to confirm the knock-out of target genes.

Generation of stable transfection cell pools

The two-plasmid packaging retroviral system was exploited to generate U2OS cells with stable transgenic expression of Myc-His-tagged WT and mutant CLOCK, and Flag-tagged WT and mutant ASS1, as well as SBP-tagged CLOCK. The pBABE and pMCB constructs with or without inserted genes were co-transfected with vectors expressing retroviral gag/pol and vsvg genes in HEK293T cells to produce retroviruses by PEI. U2OS cells were then infected by collected virus-containing culture medium, facilitated by polybrene, followed by a selection in puromycin (Sigma-Aldrich) for 4 days.

RNA interference

RNAi-mediated knock-down of CLOCK or Bmal1 was performed by transfecting siRNA oligonucleotides into U2OS or HL-7702 cells using LipofectamineRNAiMAX (Life Technologies). A non-targeting siRNA duplex was included as a negative control. The knock-down efficiency was assessed and experiments were conducted 72h after transfection. The siRNAs targeting CLOCK, Bmal1 were designed by LifeTech BLOCK-iT RNAi designer online and synthesized by Genepharma. The target sense sequences of all siRNAs used in this study are listed in the Key Resources Table.

RNA isolation and quantitative RT-PCR

Total RNA was extracted from post-confluent cells using TransZol Up reagent (TransGen Biotech, Beijing). The RNA was converted to cDNA using oligo(dT)15 and Enzyme Mix in TransScript One-Step gDNA Removal and cDNA Synthesis SuperMix kit (TransGen Biotech, Beijing). After reverse transcription, PCR reactions were performed using a ViiA7 Real-Time PCR System (Applied Biosystems) with SYBR Premix Ex Taq (TaKaRa). The PCR protocol involved denaturation at 95°C for 15 s and combined annealing and extension at 60°C for 1min over 40 cycles. The melting curve was generated after these cycles to ensure that the amplification in each reaction was specific. GAPDH was taken as internal reference. Fold changes of RNA levels were calculated using the ΔΔCt method. Primer sequences are listed in Table S2.

Immunoprecipitation, elution and western blotting

Cells or mice livers were lysed in NP-40 lysis buffer (0.25% Nonidet P-40 for Co-IP, or 0.5% for regular IP, 50mM Tris-HCl pH 7.5, 150 mM NaCl) with protease inhibitors (Sigma-Aldrich). Insoluble fraction in lysate was spinned down at 12,000rpm for 15min at 4°C to discard. For Flag immunoprecipitations, the transferred supernatant was incubated with anti-Flag M2 affinity resin (Sigma-Aldrich, A2220) for 3h at 4°C. For immunoprecipitation of endogenous ASS1, transferred supernatant was incubated with anti-ASS1 antibody (ProteinTech 16210-1-AP) at 4°C overnight, and then added with IPA300 Protein-A beads (Repligen) for 1h more incubation. After three times of washing with ice-cold NP-40 buffer, cell lysates were re-suspended with Laemmli buffer (2% SDS, 50mM Tris-HCl, pH 6.8, 10% glycerol, 5% β-mercaptoethanol, 0.0005% Bromophenol Blue) boiled at 99°C for 10min for western blotting. For ASS1 enzymatic activity assay, immunoprecipitant of ASS1-Flag was eluted in elution buffer (0.5% Triton

X-100, 50mM Tris-HCl pH 7.5, 150mM NaCl) supplemented with 0.1mg/ml FLAG peptide (Sigma-Aldrich), and then the beads were spinned down at 5,000rpm for 5min at 4°C to discard.

Either whole cell lysate samples (post-confluent cells lysed directly in Laemmli buffer) or immunoprecipitated samples were resolved by SDS-PAGE (8% or 10%) and transferred onto nitrocellulose membrane (Millipore). The membranes were incubated overnight at 4°C with corresponding primary antibodies. Membranes were then washed three times with TBST (0.05% Tween-20, 50mM Tris-HCl, pH 7.6, 150mM NaCl), incubated with horseradish peroxidase-labeled goat anti-rabbit IgG or rabbit anti-mouse IgG for 1h at room temperature, washed three times with TBST, exposed with ECL Plus (Thermo Scientific) and visualized via Typhoon Scanner (GE Healthcare).

Protein expression and purification

The pET-21b based pTEV8 constructs of His-tagged CLOCKΔN, ASS1, IMPDH2, ALDH1A1 were introduced into BL21 (DE3) *E.coli* cells. The transformants were grown at 37°C in LB medium (10 g/L tryptone, 5g/L yeast extract, 10 g/L NaCl, all from Sangon Biotech, Shanghai) untill the OD600 of medium reached 0.6. Protein expression in *E.coli* was stimulated by IPTG (Isopropyl β-D-1-thiogalactopyranoside, Sangon Biotech, Shanghai) for 16h at 16°C. *E.coli* cells were spinned down and re-suspended in TBS buffer (50mM Tris-HCl pH 7.5, 150mM NaCl) containing 5 μg/ml DNase I (New England Biolabs) and bacterial protease inhibitor cocktail (Sigma-Aldrich), then lysed in a high-pressure homogenizer (JN-3000 PLUS low temperature ultra-high pressure continuous flow cell disrupter, JNBIO), centrifuged at 12,000rpm for 15min at 4°C to remove insoluble debris. The fusion protein in the lysate was affinity-purified by Ni-NTA agarose (QIAGEN) capturing His tags after 3h incubation at 4°C. After washing with TBS supplemented with 30mM imidazole for three times, the fusion proteins were eluted by TBS supplemented with 300mM imidazole for 1h at 4°C. Purity of recombinant proteins was verified by 8% SDS-PAGE.

Protein Quantification

Concentration of purified proteins from *E.coli* or total protein in metabolite extraction samples was determined by Bradford or BCA assay kit, respectively. Relative concentration of immunoprecipitated proteins was quantified by monitoring the band intensity of western blotting by Amersham Biscience ImageQuant TL 2005v software.

GC-MS analysis for urea

Post-confluent cells were homogenized in chilled 80% (v/v) methanol. The samples were centrifuged at 12,000rpm for 10min and the supernatant was transferred to a high recovery glass sampling vial (CNW, VAAP-31509–1232-100) to vacuum dry at room temperature. The residue was oxidized with 30 μL pyridine containing 20mg/ml methoxyamine hydrochloride (Sigma-Aldrich) at 37°C overnight and further derived with 20 μL N-tert-Butyldimethylsilyl-N- methyltrifluoroacetamide (Sigma-Aldrich) at 70°C for 30min. The derived sample was injected into Aligent 7890A gas chromatography coupled to Agilent 5975C mass spectrometer. Separation was achieved on a HP-5ms fused-silica capillary column (30 m length × 250 μm ID; 5% diphenyl-95% emthylpolysiloxane bonded and crosslinked) with helium as the carrier gas at a constant flow rate of 1ml/min through the column. The temperature of front injection, MSD transfer interface and electron impact (EI) ion source were set to 280°C, 290°C and 230°C, respectively. The GC oven temperature was set to 100°C for 3 min, with an increment rate of 10°C/min to 140°C, 8°C/min to 260°C, 10°C/min to 310°C and a final 5min maintenance at 310°C. The electron impact ionization was 70eV. After 5min of solvent delay, the mass data was collected at full scan mode (m/z 50–600). Raw data was processed by MSD ChemStation based on detection and manual integration of area of peaks from individual target metabolites. Urea standard (BBI Life Sciences, Shanghai) was analyzed to determine the retention time on the column.

LC-MS analysis for metabolites

Metabolites in post-confluent cells were extracted first with 200 μL H2O (4°C), then, vortexed for 30 s and incubated in liquid nitrogen for 1min. The samples were then allowed to thaw at room temperature and sonicated for 10 min. This freeze-thaw cycle was repeated three times in total. After that, the samples were centrifuged 15min at 13,000rpm at 4°C. Each sample was extracted 20 μL supernatant to do protein quantification. The rest samples were added 720 μL ACN:MeOH (1:1, v/v), then vortexed for 30 s and sonicated for 10min. To precipitate proteins, the samples were incubated for 1h at −20°C, followed by 15min centrifugation at 13,000rpm and 4°C. The resulting supernatant was removed and evaporated to dryness in a vacuum concentrator. The dry extracts were then reconstituted in 100μl ACN:H2O (1:1, v/v), sonicated for 10min, and centrifuged 15min at 13,000rpm and 4°C to remove insoluble debris. The supernatants were transferred to HPLC vials for LC-MS analysis. The LC-MS analysis were performed using a UHPLC system (1290 series for argininosuccinate and arginine tests, 1260 series for metabolic profiling, Agilent Technologies) coupled to a triple quadruple mass spectrometer (Agilent 6495 QQQ for argininosuccinate and arginine tests, Agilent 6460 QQQ for metabolic profiling, Agilent Technologies) in the multiple reaction monitoring (MRM) mode. For the argininosuccinate and arginine tests alone, metabolites were monitored in positive mode only. For high-throughput metabolic profiling, metabolites were monitored in both ESI positive and negative modes. WATERS ACQUITY UPLC BEH Amino column (particle size, l.7 μm,100mm length x 2.1mm ID) was used for argininosuccinate and arginine tests. Phenomenex Luna amino column (particle size, 3 μm; 100mm length × 2.1mm ID) was used for metabolic profiling. The column temperature was kept at 25°C. The flow rate was 300 μl/min and the sample injection volume was 2 μl. The mobile phase A was 25mM ammonium acetate and 25mM ammonium

hydroxide in 100% water, and B was 100% acetonitrile. The linear gradient for argininosuccinate and arginine tests was set as follows: 0-1 min: 85% B, 1-6 min: 85% B to 70% B, 6-10 min: 70% B to 0% B, 10-15 min: 0% B, 15-15.1 min: 0% B to 85% B, 15.1-20 min: 85% B. The linear gradient for metabolic profiling was set as follows: 0-1 min: 85% B, 1-14 min: 95% B to 65% B, 14-16 min: 65% B to 40% B, 16-18 min: 40% B, 18-18.1 min: 40% B to 95% B, 18.1-23 min: 95% B. ESI source conditions were set as follows: sheath gas temperature, 350°C; dry gas temperature, 350°C; sheath gas flow, 12L/min for argininosuccinate and arginine tests, 11L/min for metabolic profiling; dry gas flow, 16L/min for argininosuccinate and arginine tests, 10L/min for metabolic profiling; capillary voltage, 3000V in positive mode for argininosuccinate and arginine tests, 4000V or −3500V in positive or negative modes for metabolic profiling; nozzle voltage, 1000V for argininosuccinate and arginine tests, 500V for metabolic profiling; nebulizer pressure, 40psi for argininosuccinate and arginine tests, 30psi for metabolic profiling. For argininosuccinate and arginine tests, 4 MRM transitions representing the 2 metabolites were simultaneously monitored. The dwell time for each MRM transition is 50ms, and the total cycle time is 535ms. For metabolic profiling, the dwell time for each MRM transition is 3ms, and the total cycle time is 1.263 s. Original MRM raw data was processed by MRMAnalyzer based on detection and area integration of peaks from individual target metabolites. Protein concentration was used for sample normalization. To construct the metabolite MRM library, each metabolite standard (100 μg/mL) was first analyzed in ESI positive/negative mode via flow injection using the software MassHunter Optimizer (Agilent Technologies) to get the optimal MRM transition parameters. Then the retention time (rtsingle) of each metabolite was determined by measuring the corresponding MRM transition individually on the column.

LC-MS/MS analysis for acetylation sites in ASS1

To identify residues of ASS1 acetylated by CLOCK, the ASS1 acetylated by co-incubation with CLOCKΔN in vitro was enriched with Ni-NTA agarose (QIAGEN) capturing the His tag. The affinity capture sample was subjected to SDS-PAGE and the Coomassie blue staining band corresponding to ASS1 was subjected to in-gel trypsin digestion. The resulting peptides were analyzed by Orbitrap Fusion LC-MS/MS analysis. This analysis was performed on an Easy-nLC 1000 liquid chromatography system (Thermo Fisher Scientific) connected to an LTQ Orbitrap mass spectrometer (Thermo Electron, Bremen, Germany) equipped with a nano-electrospray ion source (Thermo Fisher Scientific). Tryptic peptides were dissolved with loading buffer (5% acetonitrile and 0.1% formic acid, phase A), and then injected into homemade 2cm x 150 μm ID, C18 trap-column and subsequently eluted and separated on 12cm x 150 μm ID column (C18, 1.9 μm, 120Å) with a series of adjusted linear gradients of phase B (95% acetonitrile in 0.1% formic acid) according to the hydrophobicity of fractions, and then injected into the mass spectrometer at a constant column-tip flow rate of 500nL/min. Eluted peptides were analyzed by MS and data-dependent MS/MS acquisition. The scan range was set from m/z 300 to m/z 1400. The dynamic exclusion of previously acquired precursor ions was enabled at 18 s. Spectral data were searched against human protein RefSeq database (2013.07.01) in Proteome Discoverer 1.4.1.14 suites with Mascot software (version 2.3.01, Matrix Science) to achieve a false discovery rate of < 1%. The mass tolerance was set to be 10ppm for precursor, and it was set 0.5Da for the tolerance of product ions. Oxidation (M), Acetyl (Protein-N term), Acetyl (K), DeStreak(C) were chosen as variable modifications.

LC-MS/MS analysis for CLOCK-interacting proteins

To identify CLOCK-interacting proteins, SBP (streptavidin binding protein)-tagged human WT CLOCK was stably transfected into U2OS cells. Post-confluent cells were lysed in NP-40 lysis buffer (0.25% Nonidet P-40, 50mM Tris-HCl pH 7.5, 150mM NaCl) with protease inhibitors (Sigma-Aldrich). SBP-CLOCK was affinity captured by Streptavidin Sepharose High Performance beads (GE Healthcare) and digested by trypsin on beads after three times of washing with NP-40 lysis buffer. The resulting peptides were analyzed by Orbitrap Fusion LC-MS/MS analysis. This analysis was performed on an LC-20AB system (Shimadzu, Tokyo, Japan) connected to an LTQ Orbitrap mass spectrometer (Thermo Electron, Bremen, Germany) equipped with a nano-electrospray ion source (Michrom Bioresources, Auburn, CA). Tryptic peptides were dissolved with loading buffer (5% acetonitrile and 0.1% formic acid, phase A), and then injected into the trap-column and subsequently eluted and separated on a 15cm length x 100 μm ID reverse phase column (Michrom Bioresources, Auburn, CA) with a gradient of 5% to 45% phase B (95% acetonitrile in 0.1% formic acid) over 130min, and then injected into the mass spectrometer at a constant column-tip flow rate of 500nL/min. Eluted peptides were analyzed by MS and data-dependent MS/MS acquisition. The scan range was set from m/z 350 to m/z 1800. The dynamic exclusion of previously acquired precursor ions was enabled at 60 s. Spectral data were searched against Swiss-Prot database (Swissprot rat version 090303 with 7302 entries) by SEQUEST with PeptideProphet software to achieve a false discovery rate of < 0.9%. The mass tolerance was set to be 10ppm for precursor, and it was set 1Da for the tolerance of product ions.

In vitro acetylation assay

Our assay is modified from a previous report (de Boor et al., 2015). Recombinant ASS1, IMPDH2, Histone 3 or ALDH1A1 (1 μg) was incubated with or without CLOCK (0-2 μg, amount indicated in text/figures) in 50 μL of reaction buffer (50mM Tris-HCl pH 8.0, 10% glycerol (v/v), 0.1mM EDTA, 1mM DTT) containing 50 μM Acetyl-CoA. After 1h (or other duration indicated in text/figures) at 30°C, samples were subjected to SDS-PAGE and western blotting.

ASS1 activity assay

Our assay is modified from a previous report (Guerreiro et al., 2009). ASS1 (5 μL of in vitro acetylation reaction, equal to 0.1 μg ASS1, or 5 μL immunoprecipitated and eluted Flag-tagged ASS1) was added into 45 μL reaction Buffer (20mM Tris-HCl, pH 7.8, 2mM ATP,

6mm MgCl2, 20mM KCl) containing 0.05U of pyrophosphatase (New England Biolabs) and substrates (2mM citrulline, 2mM aspartate) in each well of 96-wells plate. The control reaction with same components but without substrates was also set. After 30min incubation at 37°C, the reaction was stopped by adding 5 μL of MG Acidic Solution (Malachite Green Phosphate Assay Kit, Cayman Chemical), mixed by gently tapping, and incubated for 10min at room temperature. After addition of 15 μL of MG Blue Solution (Malachite Green Phosphate Assay Kit, Cayman Chemical), mix by gently tapping, and incubate for 20min at room temperature, absorbance at 620nm was determined in ELx800 absorbance microplate reader (BioTek Instruments). Relative ASS1 activity was calculated as the net value deducing control reaction value from total value, normalized by ASS1 protein amount when eluted sample was used.

Cell proliferation assay

The cells were seeded into 96 well plates with initial population of 5,000 cells/well. Each cell type was seeded for 10 wells as repeats. The confluency of attached cells on the bottom of wells was monitored in IncuCyte Live-Cell Analysis System (Essen Bioscience) every hour after starting the record. Data from every 12 hr was used to generate the proliferation curve.

QUANTIFICATION AND STATISTICAL ANALYSIS

Group data are presented as mean ± SD. Comparisons between two groups were made by Student's paired or t tests. The statistical parameters are reported in figure legends or text of results. P values less than 0.05 were considered significant. Analyses were performed using the Microsoft Excel.